Unclassified
SECURITY CLASSIFICATION OF THIS PAGE

AD-A236 487

REPORT DOCUMENTATION PAGE

)188

1a. REPORT SECURITY CLASSIFICATION Unclassified	1b. RESTRICTIVE MARKINGS None
2a. SECURITY CLASSIFICATION AUTHORITY	3. DISTRIBUTION/AVAILABILITY OF REPORT Unlimited Approved for public release, distribution unlimited
2b. DECLASSIFICATION/DOWNGRADING SCHEDULE	
4. PERFORMING ORGANIZATION REPORT NUMBER(S)	5. MONITORING ORGANIZATION REPORT NUMBER(S) AFOSR-TR- 91 0509
6a. NAME OF PERFORMING ORGANIZATION Michigan State University 6b. OFFICE SYMBOL (If applicable)	7a. NAME OF MONITORING ORGANIZATION AFOSR/NA
6c. ADDRESS (City, State, and ZIP Code) East Lansing, MI 48824	7b. ADDRESS (City, State, and ZIP Code) Bolling Air Force Base Building 410 Washington, DC 20332-6448
8a. NAME OF FUNDING/SPONSORING ORGANIZATION AFOSR/NA 8b. OFFICE SYMBOL (If applicable) NA	9. PROCUREMENT INSTRUMENT IDENTIFICATION NUMBER AFOSR - 87 - 0332
8c. ADDRESS (City, State, and ZIP Code) Bolling Air Force Base Building 410 Washington, DC 20332-6448	10. SOURCE OF FUNDING NUMBERS PROGRAM ELEMENT NO. 61102F; PROJECT NO. 2307; TASK NO A2; WORK UNIT ACCESSION NO

11. TITLE (Include Security Classification)
Effects of External Forcing on Entrainment Ratio and Fluid Composition in Turbulent Shear Layers

12. PERSONAL AUTHOR(S)
M.M. Koochesfahani and C.G. MacKinnon

13a. TYPE OF REPORT	13b. TIME COVERED	14. DATE OF REPORT (Year, Month, Day)	15. PAGE COUNT
Final Technical Report	FROM 9/1/87 TO 8/31/90	1991, February, 14	52

16. SUPPLEMENTARY NOTATION

17. COSATI CODES			18. SUBJECT TERMS (Continue on reverse if necessary and identify by block number)
FIELD	GROUP	SUB-GROUP	Turbulence, Mixing Layer, Shear Flow

19. ABSTRACT (Continue on reverse if necessary and identify by block number)

The effect of forcing on mixing was documented by measuring the probability density function (pdf) of the concentration field in a nonreacting liquid shear layer forced by 2-D disturbances. The concentration field was measured using the laser induced fluorescence (LIF) technique in the passive scalar mode. Results show that composition distribution of mixed fluid in forced shear layers is essentially uniform across the width of the shear layer similar to previous results in natural layers. Forcing changes both the amount and the composition of mixed fluid. For the cases studied, forcing results in an increase of the total amount of mixed fluid (integrated across the layer width) and a shift of the predominant mixed-fluid concentration to larger values. The increase in the amount of mixing in the forced layer appears to be mostly due to the increase in the layer width and not so much the result of improved small-scale mixing. Details of the forcing waveform shape have a significant influence on the structure of the flow and the mixing field.

(continued on back)

20. DISTRIBUTION/AVAILABILITY OF ABSTRACT ☒ UNCLASSIFIED/UNLIMITED ☒ SAME AS RPT ☐ DTIC USERS	21. ABSTRACT SECURITY CLASSIFICATION Unclassified
22a. NAME OF RESPONSIBLE INDIVIDUAL Dr. James M. McMichael	22b. TELEPHONE (Include Area Code) (202) 767-4936 22c. OFFICE SYMBOL AFOSR/NA

DD Form 1473, JUN 86 *Previous editions are obsolete.* SECURITY CLASSIFICATION OF THIS PAGE

UNCLASSIFIED

1. INTRODUCTION

The objective of this research program was to determine how the imposition of two-dimensional external disturbances affects the mixing field in plane two-stream shear layers. Our study relates to the effects of forcing on mixing of species, the kind of mixing that is necessary for chemical reaction and combustion. This is in contrast to many previous investigations of forced shear layers which have concentrated on the effects of forcing as it relates to the momentum transport properties of the turbulent region [1-6]. These properties typically include the layer growth rate, mean and rms velocity field, and turbulent stresses.

The major part of this effort involved the quantification of the mixed-fluid concentration field, in terms of its probability density function (pdf), in actively forced shear layers using laser induced fluorescence (LIF) diagnostics. In a separate smaller effort, the effect of curvature on the 2-D structure of the shear layer was investigated. While the main goal is to understand the basic fluid mechanical phenomena in each case, it is hoped that the knowledge gained can be used in devising active and passive means to modify/control the flow and the mixing field. In the sections that follow, a short summary of our main results to date are presented. The details are attached as Appendices A and B.

2. SUMMARY OF RESULTS

2.1 Composition of Mixed Fluid in a Forced Shear Layer

To document the effect of forcing on mixing, a series of experiments were performed where the probability density function (pdf) of the concentration field was measured under different forcing conditions. The experiments were conducted in a gravity-driven liquid shear layer facility where forcing was achieved by oscillating one of the two free-stream velocities using an oscillating bellows mechanism in one of the supply lines. The mixing field was measured using the laser induced fluorescence (LIF) technique in the passive scalar mode. The technique is essentially the same as that developed previously by Koochesfahani and Dimotakis [7], but extended to two dimensions. Using laser sheet illumination, a 2-D CCD image array, and high speed digital image acquisition techniques, whole-field concentration data were obtained simultaneously over a grid of 512x480 points in a plane with high spatial and temporal resolution. The success of this portion of our work was in part due to a high-speed digital image acquisition system obtained through the DURIP equipment

grant (AFOSR-89-0130).

The main conclusions from a shear layer forced by 2-D disturbances are summarized below:

- Composition distribution of mixed fluid in forced shear layers is essentially uniform across the width of the shear layer similar to previous results in natural layers.
- Forcing changes both the amount and the composition of mixed fluid. For the cases studied, forcing results in an increase of the total amount of mixed fluid (integrated across the layer width) and a shift of the predominant mixed-fluid concentration to larger values.
- The increase in the amount of mixing in the forced layer appears to be mostly due to the increase in the layer width and not so much the result of improved small-scale mixing.
- Details of the forcing waveform shape have a significant influence on the structure of the flow and the mixing field. Asymmetric (i.e. nonsinusoidal) forcing can result in a much larger change in the composition field than that due to sinusoidal forcing.

The details of these findings along with the full description of the work were presented in a paper at the IUTAM Symposium on *Fluid Mechanics of Stirring and Mixing* in August 1990 in La Jolla, California [8]. This paper, attached as Appendix A, has been accepted for publication in Physics of Fluids A and will appear in April 1991. This work also forms the major part of the M.S. thesis of Mr. Colin MacKinnon.

Our study of shear layer forcing with asymmetric waveform has recently lead to interesting new results. We have reported earlier [8, 9] that asymmetric forcing with a waveform of symmetry S = 70% results in a much larger growth rate and mixed-fluid composition modification than sinusoidal (S = 50%) forcing. Asymmetric forcing with S = 30%, however, produces a "forced" shear layer which is quite similar to a "natural" layer [9]. In an ongoing effort, we have found that the similarity applies to both the layer growth and the mixing characteristics (e.g. amount of mixed fluid). Upon closer examination, it was noted that the two cases of S = 30% and 70% have identical frequency contents comprising of basically a fundamental and a subharmonic (8 and 4 Hz in this case). The main difference between the two waveforms is the phase between the fundamental and subharmonic; the fundamental-subharmonic phase for S = 30% is 180 degrees apart from that for S = 70%. The

importance of the phase between fundamental and subharmonic to the evolution of the shear layer beyond the splitter plate tip has been known for some time [5, 10, 11]. Most of these studies seem to have concentrated on the initial instability region of the shear layer where the fundamental frequency corresponds to the initial shear layer most amplified frequency. Our results support the notion that similar phenomena may occur in the case of the turbulent shear layer farther downstream. In this case, the fundamental frequency would correspond to the local natural (i.e. vortex passage) frequency of the turbulent shear layer. Further work is necessary to clarify the details of the processes involved.

2.2 Effect of Curvature on a Two-Stream Shear Layer

The extensive body of knowledge which exists on turbulent flow curvature effects concentrates on the characterization of the velocity field (see, for example, Ref. 12) whereas much less is known about the mixing field. Besides the inherent interest in curvature effects on fluid mechanics phenomena, use of curvature as a possible tool for mixing control needs to be investigated. Curvature could change the mixing field by modifying the overall large scale (2-D) entrainment into the flow and also by changes in the 3-D structure of the flow due to the Taylor-Goertler instability.

We performed a joint theoretical and experimental investigation of curvature effects on the 2-D structure of the shear layer. The inviscid, linear, parallel-flow stability analysis of spatially growing disturbances was utilized to study the instability characteristics of a curved shear layer. To study curvature effects experimentally, our shear layer facility was modified to accommodate a curved test section. Experiments involved LIF flow visualization of the mixing pattern in both natural and forced curved shear layers. Experiments and stability analysis lead to the conclusion that the effect of curvature (positive or negative) on the 2-D structure of the flow is minimal even at very small curvatures. Details of this work were reported in an earlier progress report [9] which is included here as Appendix B.

Our results to date indicate that curvature may not play any major role in modifying the initial development of the shear layer vortices and the fluid entrained into them. The influence of curvature on streamwise vorticity is known to be very strong, however. How this affects the molecular mixing field requires a more extensive investigation.

3. REFERENCES

1. Wygnanski, I., Oster, D. and Fiedler, H. [1979] "A forced, turbulent mixing-layer: A challenge for the predictor," **Turbulent Shear Flows 2**, *2nd International Symposium on Turbulent Shear Flows*, July 2-4, 1979, Springer 1980, 314-326.
2. Zaman, K. B. M. Q. and Hussain, A. K. M. F. [1981] "Turbulence suppression in free shear flows by controlled excitation," *J. Fluid Mech.*, **103**, 133-159.
3. Ho, C-M. and Huang, L-S. [1982] "Subharmonics and vortex merging in mixing layers," *J. Fluid Mech.*, **119**, 443-473.
4. Oster, D. and Wygnanski, I. [1982] "The forced mixing layer between parallel streams," *J. Fluid Mech.*, **123**, 91-130.
5. Ho, C-M. and Huerre, P. [1984] "Perturbed free shear layers," *Ann. Rev. Fluid Mech.*, **16**, 365-424.
6. Koochesfahani, M. M. and Dimotakis, P. E. [1989] "Effects of a downstream disturbance on the structure of a turbulent plane mixing layer," *AIAA J.*, **27(2)**, 161-166.
7. Koochesfahani, M. M. and Dimotakis, P. E. [1985] "Laser induced fluorescence measurements of mixed fluid concentration in a liquid plane shear layer," *AIAA J.*, **23(11)**, 1700-1707.
8. Koochesfahani, M. M. and MacKinnon, C. G. [1990] "Influence of forcing on the composition of mixed fluid in a two-stream shear layer," Presented at the *IUTAM Symposium on Fluid Mechanics of Stirring and Mixing*, La Jolla, California, 20-24 August, 1990; Accepted for publication in *Phys. Fluids A* (to appear April 1991).
9. Koochesfahani, M. M. and MacKinnon, C. G. [1990] "Effects of external forcing on entrainment ratio and fluid composition in turbulent shear layers," AFOSR-87-0332 Annual Progress Report, 20-March-1990.
10. Monkewitz, P. A. [1988] "Subharmonic resonance, pairing and shredding in the mixing layer," *J. Fluid Mech.*, **188**, 223-252.
11. Hajj, M., Miksad, R. and Powers, E. [1991] "Experimental investigation of the fundamental-subharmonic coupling: Effect of the initial phase difference," AIAA-91-0624.
12. Wang, C. [1984] "The effects of curvature on turbulent mixing layers," Ph.D. Thesis, California Institute of Technology, 1984.

APPENDIX A

(To appear in *Physics of Fluids A* in April 1991)

INFLUENCE OF FORCING ON THE COMPOSITION OF MIXED FLUID IN A TWO-STREAM SHEAR LAYER

M. M. Koochesfahani * and C. G. MacKinnon #

Michigan State University
East Lansing, Michigan

The probability density function (pdf) of mixed-fluid composition in nonreacting forced liquid mixing layers is measured using laser induced fluorescence diagnostics. Results show that the composition distribution of mixed fluid in forced shear layers is essentially uniform across the width of the shear layer similar to previous results in natural shear layers. For the cases studied, forcing results in an increase of the total amount of mixed fluid (integrated across the layer width) and a shift of the predominant mixed-fluid concentration to larger values. The increase of the amount of mixing in the forced layer appears to be mostly due to the increase in the layer width and not so much the result of improved small-scale mixing. It is shown that the details of the forcing waveform shape can have a significant influence on the structure of the flow and the mixing field.

Presented as Paper PB.7 at the IUTAM Symposium on Fluid Mechanics of Stirring and Mixing, La Jolla, California, 20-24 August, 1990.

* Assistant Professor, Department of Mechanical Engineering.

Graduate Student, Department of Mechanical Engineering.

revised
12 December 1990

I. INTRODUCTION

It is well documented that forcing can be used to manipulate the evolution of turbulent mixing layers. Using a variety of techniques, it has been shown, for example, that two-dimensional perturbations may suppress or enhance the spreading rate of the shear layer [1-6]. Except for a few cases, which will be discussed shortly, virtually all experimental studies of forced shear layers to date have concentrated on the effects of forcing on mixing as it relates to the momentum transport properties of the turbulent region. These properties typically include the layer growth rate, mean and rms velocity field, and turbulent stresses. The study presented here relates to the effects of forcing on mixing of species, the kind of mixing that is necessary for chemical reactions and combustion.

We are aware of only two experimental studies where information is available on molecular mixing of species in a two-dimensionally forced shear layer. In a work by Wygnanski, et al. [1], heating was used as a passive contaminant mainly for the purpose of observing the structure of the flow. Average and rms temperature profiles were used to conclude that, in their experiment, the forced shear layer consisted of an orderly array of vortices whose core was fairly well mixed. The work of Roberts [7, 8] is the most extensive body of research on mixing in forced shear layers. Using chemically reacting techniques in a liquid-phase shear layer, he showed that the extent of molecular mixing, as manifested by the total amount of chemical product in the layer, can be altered upon shear layer forcing. All of these measurements were performed at *one* fixed value of the reactant stoichiometric ratio. It should be noted, however, that it is nearly impossible to obtain unambigous information on molecular mixing from a chemically reacting experiment at a single stoichiometric ratio. The source of the difficulty is that the amount of chemical product depends on both the *amount* and *composition* of the molecularly-mixed fluid. A full description of the effect of forcing on molecular mixing requires information on the entire composition distribution of the mixed fluid, namely the probability density function (pdf) of the concentration field. It is the purpose of this study to provide such information. We draw attention to the utility of this type of information in mixing control where manipulating a turbulent shear layer to have more mixed fluid may prove ineffective if the resulting mixed fluid has an undesirable composition.

In the current work, the pdf of the concentration field in a forced liquid shear layer is estimated using a passive scalar technique. It is known that this technique yields an upper bound to the actual molecular mixing (e.g. see Refs. 10, 11). In using this technique, a passive scalar contaminant, such as dye, is premixed with one of the streams. The concentration of dye within a small sampling volume,

determined by the spatial and temporal resolution characteristics of the measuring apparatus, is then recorded as a function of time. The difficulty arises if the sampling volume is larger than the smallest mixing (diffusion) scale, as is usually the case in high Reynolds number flows. Under these circumstances, it is impossible to determine whether the two fluids are mixed or not within the measurement resolution. For the measurements reported here, for example, the spatial resolution was estimated to be approximately 4.4 times larger than the smallest diffusion scale (see Section 2). The problem of finite sampling volume can, of course, be solved by using diagnostics that rely on chemically reacting techniques [10, 11].

With all the potential drawbacks associated with the passive scalar method in determining the true extent of molecular mixing, it nevertheless is the simplest way to get an estimate of the pdf of the composition field in a single experiment. While it is possible to determine the pdf from chemical-reaction data with much better accuracy in representing molecular mixing, this would require many experiments at different reaction stoichiometric ratios. The results presented in this paper are not intended to provide an absolute measure of the extent of mixing; as mentioned earlier, they yield an upper bound to the actual molecular mixing. The primary focus of these results is to characterize the *relative* changes in the pdf of the composition field in a forced shear layer compared to a base state (the natural layer, in this case). We believe such comparisons are warranted since the relative resolution (compared to the diffusion scale) is essentially the same in all of these measurements.

The paper is organized as follows. Section 2 gives a brief description of the measuring technique and instrumentation. Discussion of results in Section 3 includes both sinusoidal and non-sinusoidal forms of forcing. Most of the quantities discussed are computed from the measured pdf's. The definitions of these quantities are given in the Appendix.

II. EXPERIMENTAL FACILITY & INSTRUMENTATION

Experiments were conducted in a gravity-driven water shear layer apparatus in which the free-stream fluids were supplied from two independent reservoirs (see Figure 1). The test section had a cross section of 4 cm (height) x 8 cm (span) and was 35 cm long. Forcing was achieved by oscillating the high-speed free-stream speed using an oscillating bellows in the high-speed stream supply line as shown in Figure 2. The motion of the bellows was controlled by a shaker coil mechanism whose command signal originated from a function generator (HP3314A).

For the results described here, the free-stream speeds were set to $U_1 = 40$ cm/s and $U_2 = 20$ cm/s. The natural shear layer roll-up frequency F_o, under these conditions was about 27 Hz. The bellows was driven sinusoidally at frequencies of $F = 4$, 8 Hz. In the case of 4 Hz, a skewed sine wave motion was also used in order to observe the effect of nonsinusoidal forcing. In this case, we characterize the bellows motion in terms of the symmetry parameter S, which is the percentage of a period (in one cycle) during which the bellows is moving in the downward (i.e. increasing free-stream speed) direction. Results are presented for $S = 70\%$ ($F = 4$ Hz). Note that $S = 50\%$ corresponds to sinusoidal forcing. The rms velocity fluctuation imposed on the high-speed stream as a result of forcing was estimated to be $\leq 0.5\%$.

The mixing field was measured using the laser induced fluorescence (LIF) technique described by Koochesfahani & Dimotakis [9, 11]. A fluorescent dye (disodium fluorescein) was premixed with the low-speed free-stream fluid which was subsequently diluted in the shear layer as a result of mixing with the fluid from the high-speed free stream. Recording the fluorescence intensity allowed a quantitative measurement of the dye concentration and, therefore, the relative concentration of high-speed to low-speed fluid in the layer. This was done by noting that the local instantaneous dye concentration C_d in a sampling volume is given by

$$C_d = C_{d_o} \frac{\upsilon_2}{\upsilon_1 + \upsilon_2}$$

where C_{d_o} is the free-stream dye concentration carried by the fluid on the low-speed side and υ_1 and υ_2 are the volumes of fluid from the high-speed and low-speed streams, respectively, in the sampling volume. The normalized concentration of high-speed fluid ξ is thus equal to

$$\xi = 1 - C_d / C_{d_o}$$

where $\xi = \upsilon_1/(\upsilon_1 + \upsilon_2)$ is defined as the high-speed fluid volume fraction.

The LIF measurements were carried out over a plane defined by a laser sheet aligned along the flow direction at the shear layer midspan location. The laser sheet (thickness about 0.5 mm) was formed by passing the beam of a 4 W argon-ion laser (EXCEL-3000) through a combination of spherical and cylindrical lenses. The fluorescence intensity was recorded by a 2-D CCD camera (NEC TI-24A) operating at 60 fields/s with an exposure of 2 msec. The 4 cm width of the test section was imaged on 200 pixels (out of 480 vertical pixels available) of the camera so that the spatial resolution was 200 μm x 200 μm. At this resolution, the 512 horizontal pixels of the camera allowed measurements along 10.24 cm of the flow in the streamwise direction.

The camera output was digitized to 8 bits at full video rate into hard disk in real time by a digital image acquisition system (TRAPIX-5500). Note that, with this arrangement, simultaneous multipoint measurements of species concentration were obtained at 512 x 480 grid points (512 x 200 pixels inside test section) as a function of time with high spatial (200 μm x 200 μm) and temporal (2 msec) resolution. For each run, 256 sequential LIF images (i.e. 64 MBytes of data) were acquired to construct the pdf and also allow the monitoring of the spatiotemporal evolution of the concentration field in two dimensions. The number of structures passing the field of view during the data acquisition period was approximately 34 for the case of forcing at 4 Hz and 68 for forcing at 8 Hz.

The steps for processing the fluorescence intensity data are described in detail by Koochesfahani & Dimotakis [9] and are not repeated here. We should mention that in the present experiments the laser intensity attenuation due to absorption by the dye was negligible; the non-uniformity in the laser sheet illumination and camera pixel sensitivity were taken into account, however.

For the measurements presented here, the region of the flow between 15 cm $< x <$ 25 cm was imaged on the camera. At the middle of this region (i.e. at x = 20 cm), the local natural shear layer width δ_1 (see Appendix) was estimated to be about 3.3 cm, resulting in a local Reynolds number of 6,600. This Reynolds number corresponds to a natural shear layer during the mixing transition [10]. Recent results by Miller and Dimotakis [12] indicate that the smallest expected scalar diffusion scale (Batchelor scale) λ_D is very close to the Kolmogorov scale λ_K in water where the Schmidt number is approximately 600. Schmidt number, $Sc = \nu/D$, is the ratio of the diffusion coefficient of momentum to that of mass. Estimating the

Kolmogorov scale by $\lambda_K \simeq \delta_1 \mathrm{Re}^{-\frac{3}{4}}$, gives a value for the smallest diffusion scale $\lambda_D \simeq 45$ μm for the conditions at $x = 20$ cm mentioned above. As discussed in the introduction, our results provide an upper bound to the actual molecular mixing since the typical spatial resolution of these measurements is about 4.4 times larger than the smallest mixing scale. The characterization of the relative changes in the pdf of the composition field in a forced shear layer compared to the natural layer is expected to be reliable, however, since the relative resolution (compared to the diffusion scale) is basically the same in all of these measurements.

III. RESULTS & DISCUSSION

Typical digital planar LIF data for natural and forced shear layers are presented in Figures 3 through 6. Each figure shows a time sequence (Δt = 1/15 sec) of the mixing field over a downstream region 15 cm < x < 25 cm. These time sequences represent less than 1% of the data available for a given run. Flow is from right to left with the high-speed stream on top. At each time step, the image is actually composed of 50,000 (200 in y and 500 in x) pixels. Colors are assigned to different mixed fluid concentration levels in order to aid the interpretation of data. The color assignments are as follows:

$0.88 \le \xi < 0.94$ Red	$0.64 \le \xi < 0.70$ Dark green
$0.82 \le \xi < 0.88$ Orange	$0.58 \le \xi < 0.64$ Purple
$0.76 \le \xi < 0.82$ Yellow	$0.52 \le \xi < 0.58$ Blue
$0.70 \le \xi < 0.76$ Green	$0.40 \le \xi < 0.52$ White
	$0.28 \le \xi < 0.40$ Crimson

Concentration levels below 0.28 were not labeled since the probability of their occurence was relatively low. Note also that pure fluids from the high-speed (ξ = 1) and low-speed (ξ = 0) streams were not assigned colors and appear black.

Figures 3-5 show the enhanced growth rate of the sinusoidally forced shear layer compared to the natural case. This observation is consistent with previous results [3,4,6] establishing the large increase of layer growth rate under low-frequency (relative to natural frequency F_o) forcing. Additionally, present results indicate that using a nonsinusoidal form of forcing can lead to even larger growth rates; compare Figures 5 and 6. In the case of sinusoidal forcing (S = 50%) at 4 and 8 Hz, we see a single large scale vortex lump passing through the middle of the field of view (x = 20 cm). For the particular form of nonsinusoidal forcing used here (F = 4 Hz, S = 70%), the flow is characterized by large pairing vortices convecting through the field of view (Fig. 6). Note that the size of the structures in these forced layers has become comparable to the test section height. It is quite possible that the finite height of the test section may be interfering with the growth and evolution of the structures. This is particularly serious in the case of F = 4 Hz, S = 70% where the bottom side of the structures actually comes in contact with the lower wall of the test section at some downstream distance.

From the image time series discussed above, the probability density function (pdf) of the concentration field can be constructed at any of the 50,000 measurement points in the (x, y) plane. For the remainder of this paper, we will discuss the

results only at x = 20 cm (i.e. midway between the left and right edges of the LIF images in Figures 3-6). These results can be considered representative because of the small variation of the pdf's over the range of streamwise locations investigated here. Note that the descriptions of the quantities discussed below and how they are computed from the pdf's are included in the Appendix.

The composition distribution for natural and forced (F = 4 Hz) shear layers are shown in Figure 7(a-c) in terms of the contour plot of the pdf, $p(\xi, y)$, at x = 20 cm. One main feature is apparent in this figure: in all cases, the composition distribution of mixed fluid is uniform across the width of the shear layer. This is also true for the case of F = 8 Hz whose pdf was not included in Figure 7. The uniformity of mixed-fluid composition in natural shear layers, known for some time now (e.g. see Refs. 9, 11, 16), is an attribute of the vortical motion of the large scale structures. That similar results also apply to forced shear layers is, therefore, not surprising. These findings are consistent with the recent direct numerical simulation of mixing in a forced shear layer by Buell & Mansour [13].

One advantage of the uniformity of mixed-fluid pdf is that the composition field of the whole layer can be characterized by a total pdf, $P(\xi)$, which is the integral of $p(\xi, y)$ across the width of the layer (see Appendix). The total pdf's, presented in Figure 8, illustrate the main effects of forcing on the mixing field. Note that forcing changes both the amount and the composition of the mixed fluid. For the cases we have studied thus far, the predominant concentration shifts to larger values, namely mixing is enhanced preferentially at higher values of ξ. Visual inspection of the total pdf's suggests that the total amount of mixed fluid in the layer has increased upon forcing; quantitative measure will be presented later. An interesting result is that the details of the forcing waveform shape have a significant influence on the structure of the flow, as discussed earlier, and the mixing field. Figure 8b shows that asymmetric forcing (i.e. nonsinusoidal) can result in a much larger change in the composition field than that due to sinusoidal forcing. This can also be visually confirmed by observing the increased amount of high concentration fluid (i.e. red, orange, yellow colors) in Figure 6 compared to Figure 3.

As was discussed above, in all forcing cases presented here the predominant mixed-fluid composition shifts to larger values. This may be interpreted to be due to an increased asymmetry of the entrainment ratio into the shear layer. It is known that the natural shear layer entrains an unequal amount of fluid from the two free streams. The entrainment ratio E is defined to be the volume ratio of the entrained high-speed to low-speed fluids. In the recent model of entrainment by Dimotakis [14], the geometric properties of the large-scale flow structures of the natural mixing layer were utilized to derive an expression for the entrainment ratio. For the case of

uniform density, the expression was given as $E = 1 + 3.9\,\delta_\omega/x$, where δ_ω is the vorticity thickness. This expression connects the entrainment ratio directly to the layer growth rate. The equivalent relationship applicable to forced layers has not been established to our knowledge and whether the expression for natural shear layer entrainment ratio can be applied to forced layers remains to be proven. We note, however, that compared to the natural layer, the forced shear layers studied here have larger growth rates; they also have higher values of predominant mixed-fluid concentration.

The pdf of the composition field $p(\xi, y)$ can be used to calculate the transverse profiles of some quantities of interest (see Appendix). The reference location $y = 0$ and local layer thickness δ_1 used in these profiles were determined according to the description in the Appendix. The average concentration $\bar{\xi}(y)$ is shown in Figure 9. The profiles for forced conditions develop a "flat" region similar to that observed by Wygnanski, et al. [1], who attributed this feature to an orderly array of vortices with fairly well mixed cores. The probabilities of finding unmixed fluid from low- and high-speed streams, $p_o(y)$ and $p_1(y)$ respectively, are displayed in Figure 10. Note the large increase in the probability of finding unmixed fluid (from both streams) in the middle of the layer as forcing is applied. Examining the LIF images in Figures 3 through 6 leads to the conclusion that the increase is due to the more pronounced and larger entrainment tongues between the large structures in the forced layer. Correspondingly, the total probability of finding mixed fluid $p_m(y)$ in Figure 11 shows a decrease in the middle of the forced shear layer, indicating a reduction in the amount of mixed fluid.

As a measure of the total amount of mixed fluid across the layer, the mixed-fluid thickness δ_m was calculated. This measure is essentially the area under the $p_m(y)$ curve. The table below compares the total amount of mixed fluid across the layer and also the amount per unit width of the layer for the cases investigated.

	δ_m (mm)	δ_m / δ_1
Natural	16.1	0.48
F = 8 Hz, S = 50%	19.3	0.51
F = 4 Hz, S = 50%	18.3	0.45
F = 4 Hz, S = 70%	19.7	0.43

The most important result is that while the total amount of mixed fluid in the forced layer has increased by as much as 22%, the amount of mixing per unit width of the layer has remained nearly constant. This suggests that the forced layers in our study

have more mixed fluid mostly by virtue of the increased local width of the layer and not so much because of improved small scale mixing. In fact, as noted earlier, there is less mixed fluid in the center of a forced shear layer compared to the natural layer.

The effect of 2-D forcing on the development of 3-D small scales need to be studied in greater detail. Recent results by Huang & Ho [15] connect the production of random small-scale eddies to the interaction between the merging spanwise structures and the streamwise vortices. The present results suggest that 2-D forcing may not lead to any increase of small scale mixing. It is not clear whether this is true for all forced shear layers. In particular, we do not have any information on the effects of forcing amplitude on the mixing field. Furthermore, much work still remains to understand how the frequency contents (i.e. shape) of forcing waveform affect the large and small scales in a turbulent shear layer.

IV. CONCLUSIONS

The results presented show that the composition distribution of mixed fluid in forced shear layers is essentially uniform across the width of the shear layer similar to previous results in natural shear layers. For the cases studied, the total amount of mixed fluid integrated across the layer width increases. The amount of mixed fluid per unit width of the shear layer does not vary significantly, however. This implies that the increase of mixing in the forced layer is mostly due to the increase in the layer width and not because of improved small-scale mixing. In all the cases investigated here, mixed-fluid composition in the shear layer changes with forcing such that the predominant mixed-fluid concentration shifts to larger values. In other words, mixing is enhanced preferentially at higher values of concentration. Finally, results show that nonsinusoidal forcing can have a significant influence on the structure of the flow and the mixing field.

ACKNOWLEDGMENT

This work was sponsored by the Air Force Office of Scientific Research Grants No. AFOSR-87-0332 and AFOSR-89-0130. The expert help of Mr. Robert Schrader during the initial phase of the work is gratefully acknowledged.

APPENDIX

This section gives the definitions of the quantities discussed in this paper and how they are related to the pdf of the high-speed fluid concentration ξ. Most of these definitions are based on those described by Koochesfahani & Dimotakis [9, 11].

The pdf of ξ at a given point y in the shear layer is denoted by $p(\xi,y)$. Since the pdf is normalized, we have

$$\int_0^1 p(\xi,y)\,d\xi = 1. \tag{A1}$$

The average concentration of high-speed fluid $\bar{\xi}$ is then given by

$$\bar{\xi}(y) = \int_0^1 \xi p(\xi,y)\,d\xi. \tag{A2}$$

In the ideal case, the two 'delta' functions in $p(\xi,y)$ at $\xi = 0, 1$ are associated with the pure unmixed fluids from the low- and high-speed sides, respectively. In practice, however, the width ε of these delta functions is nonzero and is dictated by the overall signal-to-noise ratio of the measurement. In the present work, the range of ξ was divided into 21 levels so that the value of ε was about 0.047. Concentrations in the range $0 \le \xi < \varepsilon$ are assigned to pure (unmixed) low-speed fluid and $1-\varepsilon < \xi \le 1$ to pure high-speed fluid. The range $\varepsilon \le \xi \le 1-\varepsilon$ would, therefore correspond to mixed fluid. With this description, the probabilities p_o and p_1 of finding unmixed fluids from low- and high-speed sides respectively, are given by

$$p_o(y) = \int_0^{\varepsilon} p(\xi,y)\,d\xi\,, \quad p_1(y) = \int_{1-\varepsilon}^1 p(\xi,y)\,d\xi. \tag{A3}$$

The mixed-fluid pdf corresponds to the portion of $p(\xi,y)$ excluding the two delta functions. The area under the mixed-fluid pdf, p_m, gives the total probability of finding mixed fluid at *any* concentration. It is given by

$$p_m(y) = \int_{\varepsilon}^{1-\varepsilon} p(\xi,y)\,d\xi. \tag{A4}$$

A value of $p_m(y)$ of less than unity implies the presence of unmixed fluid. The reference location $y = 0$ which is used throughout this work was arbitrarily chosen to

coincide with the point at maximum $p_m(y)$. Additionally, the reference thickness δ_1 which is essentially equivalent to the layer visual thickness (see Ref. 11) was defined as the 1% width of $p_m(y)$ where p_m has dropped to 1% of its maximum value.

Since it was observed that the shape of the mixed-fluid pdf was nearly invariant across the width of the shear layer for all the cases studied, the composition field of the whole layer can be characterized by a single pdf. The total pdf integrated across the layer is given by

$$P(\xi) = \int_{-\infty}^{+\infty} p(\xi,y)\, dy, \tag{A5}$$

The total amount of mixed-fluid integrated across the shear layer width can be characterized by the mixed-fluid thickness δ_m defined by

$$\delta_m = \int_{-\infty}^{+\infty} p_m(y)\, dy = \int_{\varepsilon}^{1-\varepsilon} P(\xi)\, d\xi. \tag{A6}$$

In the case of chemically reacting shear layers, an often-used measure of the total amount of chemical product in the layer is the product thickness. For fast chemical reactions in the limit of large and small reaction stoichiometric ratios, two product thicknesses are defined as follows (see Refs. 11, 16)

$$\delta_{p_1} = \int_{-\infty}^{+\infty} \int_{\varepsilon}^{1-\varepsilon} \xi p(\xi,y)\, d\xi\, dy, \quad \delta_{p_2} = \int_{-\infty}^{+\infty} \int_{\varepsilon}^{1-\varepsilon} (1-\xi) p(\xi,y)\, d\xi\, dy. \tag{A7}$$

It is easy to show that the mixed-fluid thickness and the two product thicknesses are related by

$$\delta_m = \delta_{p_1} + \delta_{p_2}. \tag{A8}$$

We note that it is the product thickness δ_{p_2} which Roberts [7, 8] uses as the variable to describe the effect of forcing in his forced shear layer studies.

V. REFERENCES

1. Wygnanski, I., Oster, D. and Fiedler, H. [1979] "A forced, turbulent mixing-layer: A challenge for the predictor," **Turbulent Shear Flows 2**, *2nd International Symposium on Turbulent Shear Flows*, July 2-4, 1979, Springer 1980, 314-326.
2. Zaman, K. B. M. Q. and Hussain, A. K. M. F. [1981] "Turbulence suppression in free shear flows by controlled excitation," *J. Fluid Mech.*, **103**, 133-159.
3. Ho, C-M. and Huang, L-S. [1982] "Subharmonics and vortex merging in mixing layers," *J. Fluid Mech.*, **119**, 443-473.
4. Oster, D. and Wygnanski, I. [1982] "The forced mixing layer between parallel streams," *J. Fluid Mech.*, **123**, 91-130.
5. Ho, C-M. and Huerre, P. [1984] "Perturbed free shear layers," *Ann. Rev. Fluid Mech.*, **16**, 365-424.
6. Koochesfahani, M. M. and Dimotakis, P. E. [1989] "Effects of a downstream disturbance on the structure of a turbulent plane mixing layer," *AIAA J.*,**27(2)**, 161-166.
7. Roberts, F. A. [1985] "Effects of a periodic disturbance on mixing in turbulent shear layers and wakes," Ph.D. Thesis, California Institute of Technology.
8. Roberts, F. A. and Roshko, A. [1985] "Effects of periodic forcing on mixing in turbulent shear layers and wakes," AIAA-85-0570.
9. Koochesfahani, M. M. and Dimotakis, P. E. [1985] "Laser induced fluorescence measurements of mixed fluid concentration in a liquid plane shear layer," *AIAA J.*, **23**, 1700-1707.
10. Breidenthal, R. E. [1981] "Structure in turbulent mixing layers and wakes using a chemical reaction," *J. Fluid Mech.*, **109**, 1-24.
11. Koochesfahani, M. M. and Dimotakis, P. E. [1986] "Mixing and chemical reactions in a turbulent liquid mixing layer," *J. Fluid Mech.*, **170**, 83-112.
12. Miller, P. L. and Dimotakis, P. E. [1991] "Stochastic geometric properties of scalar interfaces in turbulent jets," *Phys. Fluids*, To appear January 1991.
13. Buell, J. C. and Mansour, N. N. [1989] "Asymmetric effects in three-dimensional spatially-developing mixing layers," *Seventh Symposium on Turbulent Shear Flows*, Stanford University, August 21-23, 1989, 9.2.1-9.2.6.
14. Dimotakis, P. E. [1986] "Two-dimensional shear-layer entrainment," *AIAA J.*, **24(11)**, 1791-1796.

15. Huang, L-S. and Ho, C-M. [1990] "Small-scale transition in a plane mixing layer," *J. Fluid Mech.*, **210**, 475-500.

16. Mungal, M. G. and Dimotakis, P. E. [1984] "Mixing and combustion with low heat release in a turbulent shear layer," *J. Fluid Mech.*, **148**, 349-382.

FIGURE CAPTIONS

Figure 1. Schematic of the mixing layer facility.

Figure 2. Shear layer forcing mechanism.

Figure 3. Digital LIF image time sequence of the mixing field for the natural layer. Flow is from right to left and time increases from top to bottom (Δt = 1/15 sec).

Figure 4. Digital LIF image time sequence of the mixing field for sinusoidal forcing at F = 8 Hz, S = 50%.

Figure 5. Digital LIF image time sequence of the mixing field for sinusoidal forcing at F = 4 Hz, S = 50%.

Figure 6. Digital LIF image time sequence of the mixing field for nonsinusoidal forcing at F = 4 Hz, S = 70%.

Figure 7. *Contour plot of the composition distribution* $p(\xi, y)$ at x = 20 cm,
(a) Natural; (b) Forced, F = 4 Hz, sinusoidal (S = 50%);
(c) Forced, F = 4 Hz, nonsinusoidal (S = 70%).

Figure 8. Effect of forcing on the total pdf of the concentration field,
(a) Sinusoidal forcing; (b) Nonsinusoidal forcing.

Figure 9. Transverse profile of average high-speed fluid concentration.

Figure 10. Transverse profiles of pure free-stream fluid probability,
(a) Low-speed fluid; (b) High-speed fluid.

Figure 11. Transverse profile of total mixed-fluid probability.

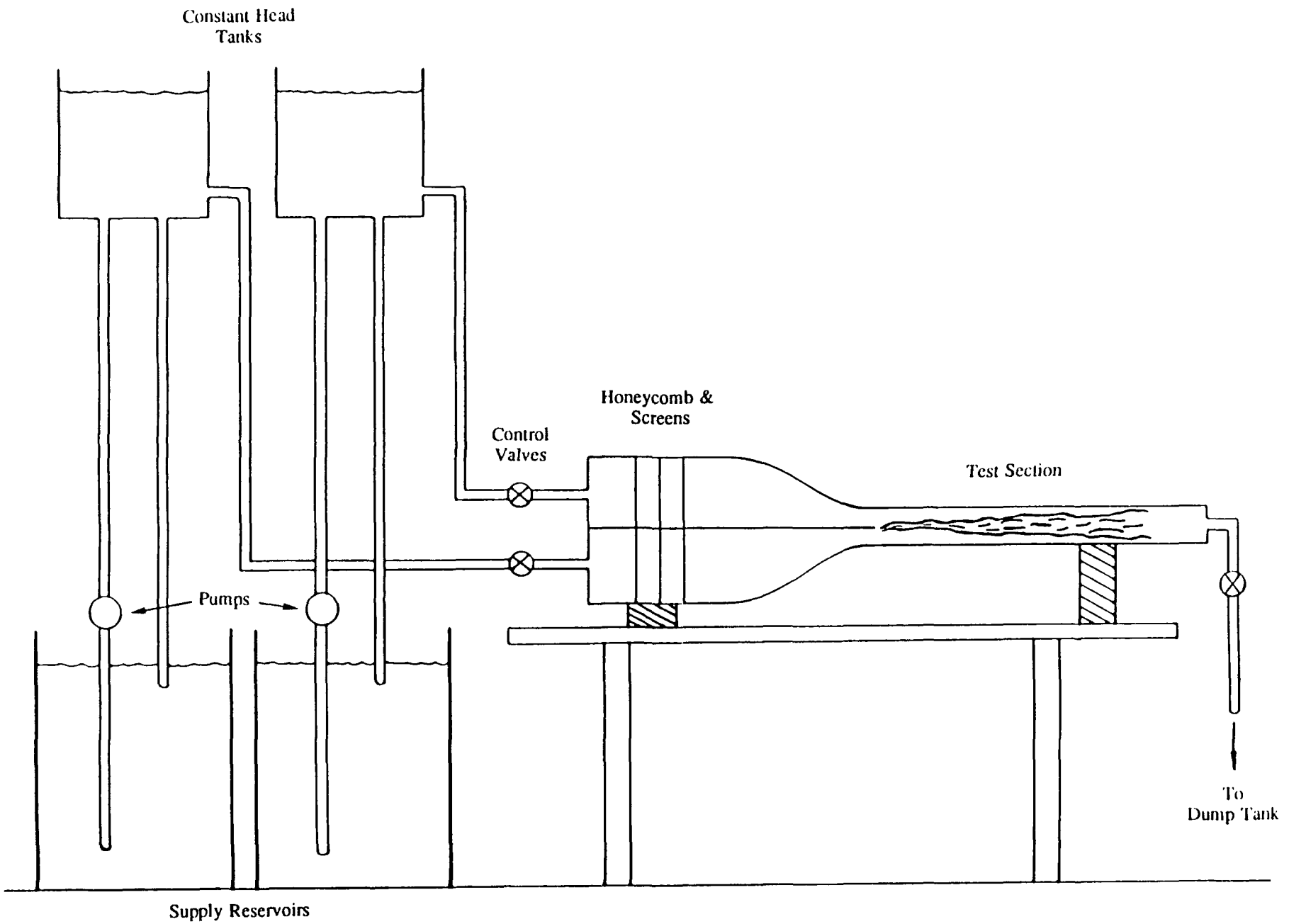
Constant Head
Tanks
Honeycomb &
Screens
Control
Valves
Test Section
Pumps
To
Dump Tank
Supply Reservoirs

Figure 1.

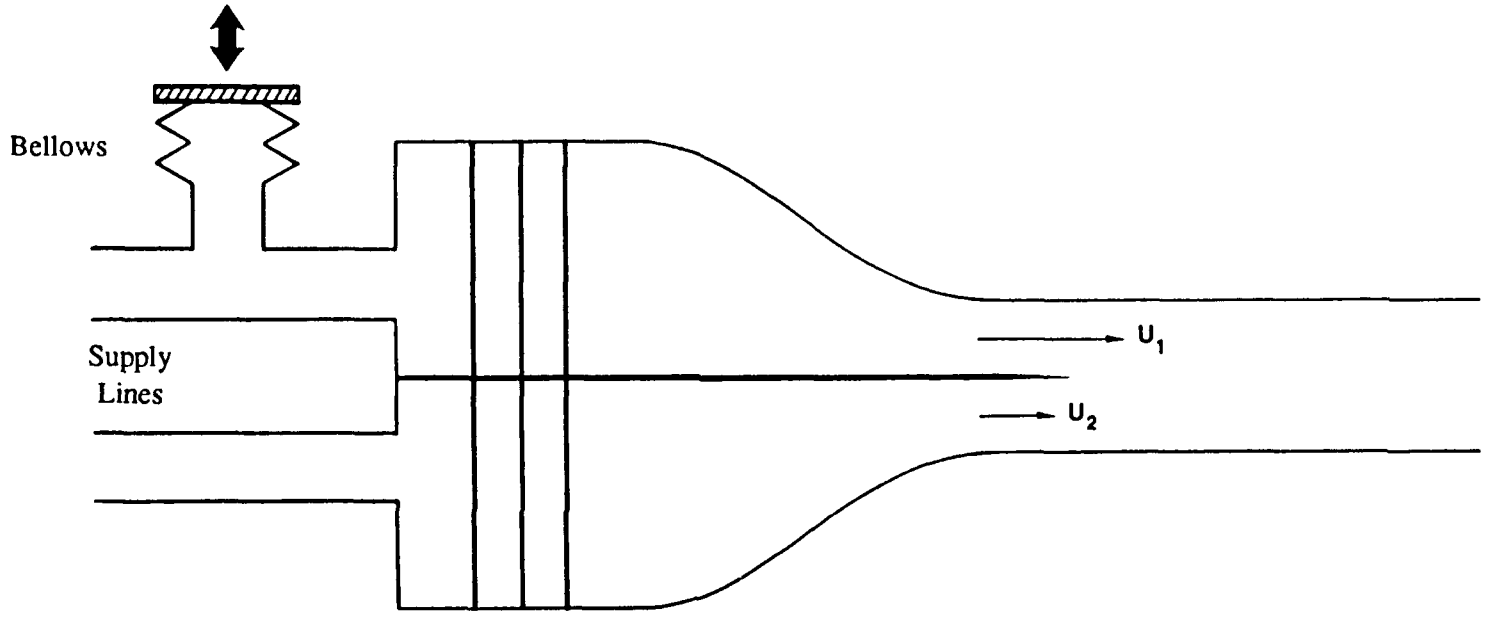

Figure 2.

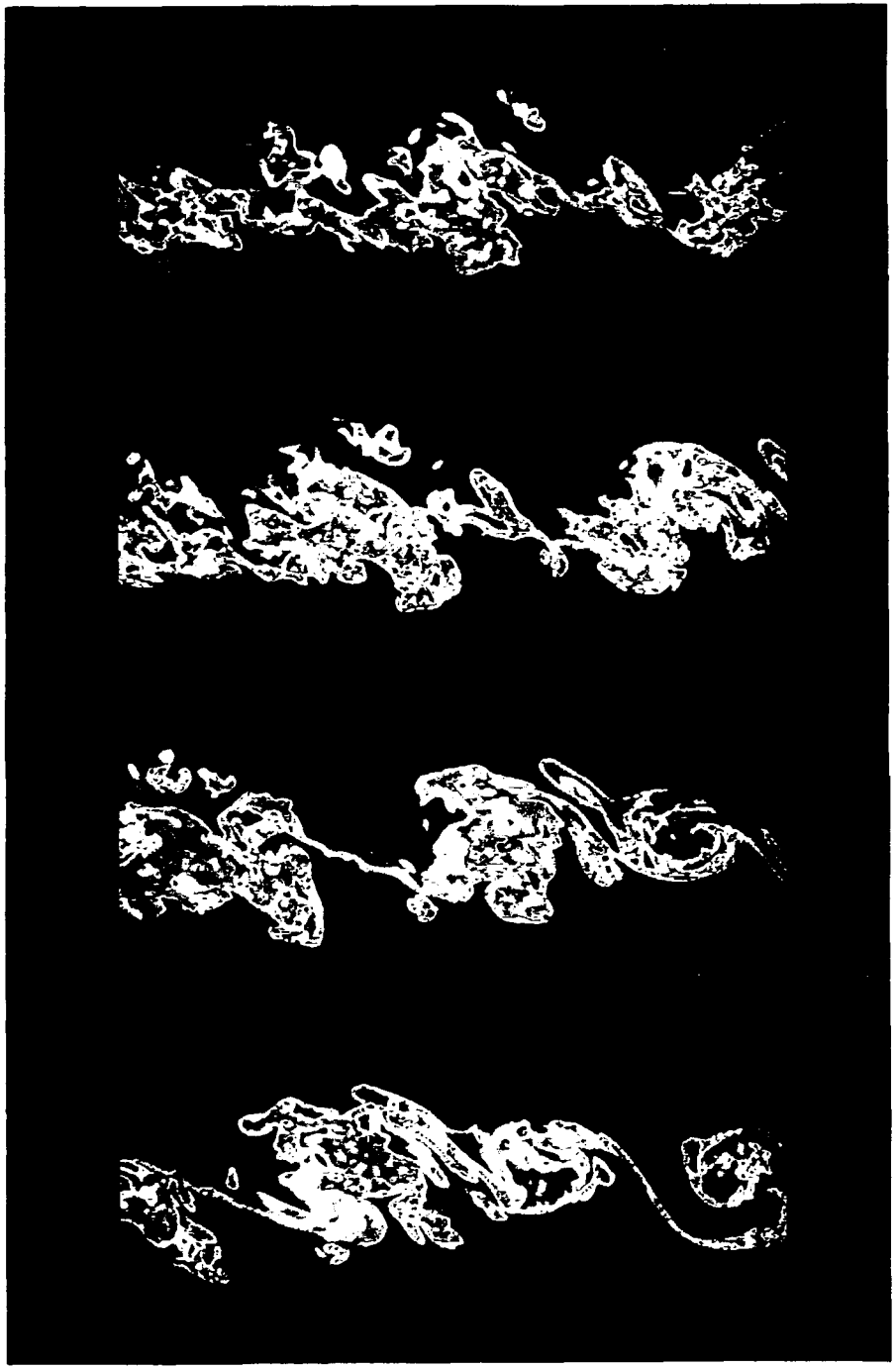

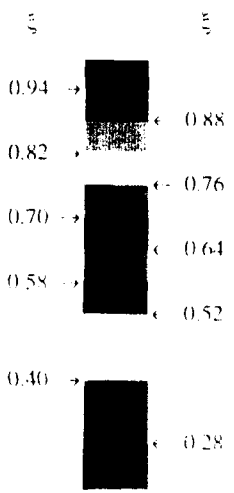

Figure 3

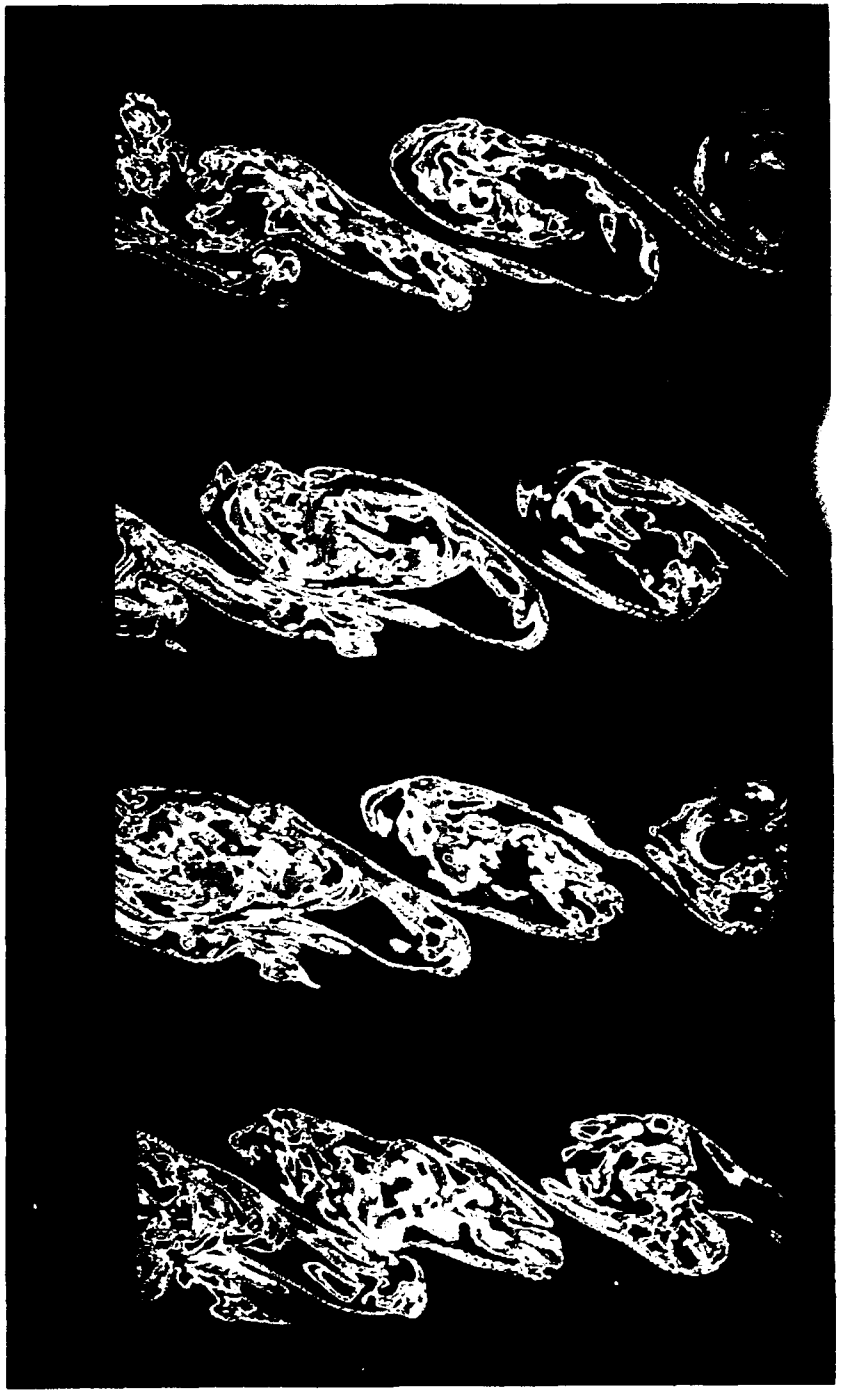

Figure 4.

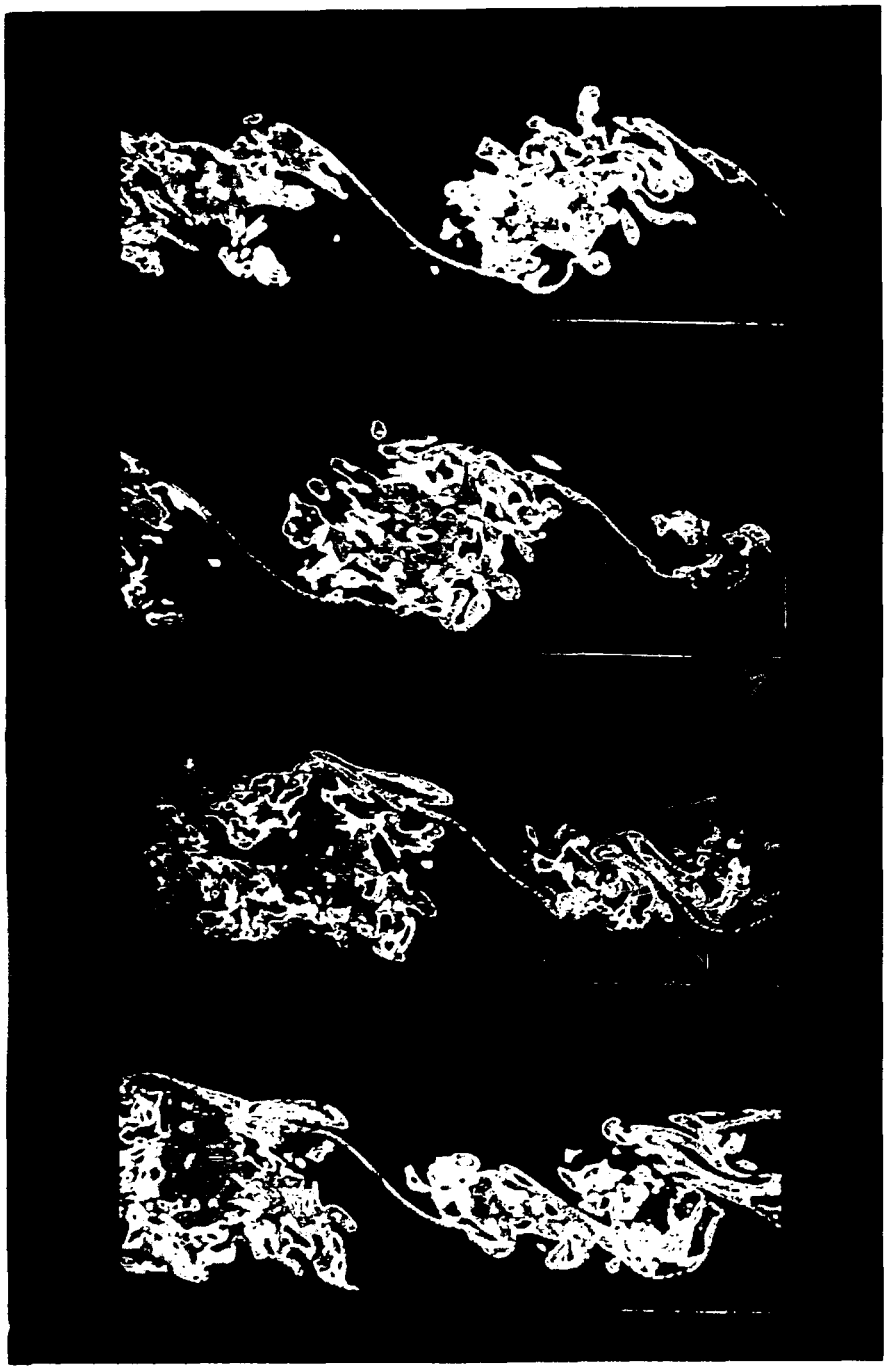

Figure 5

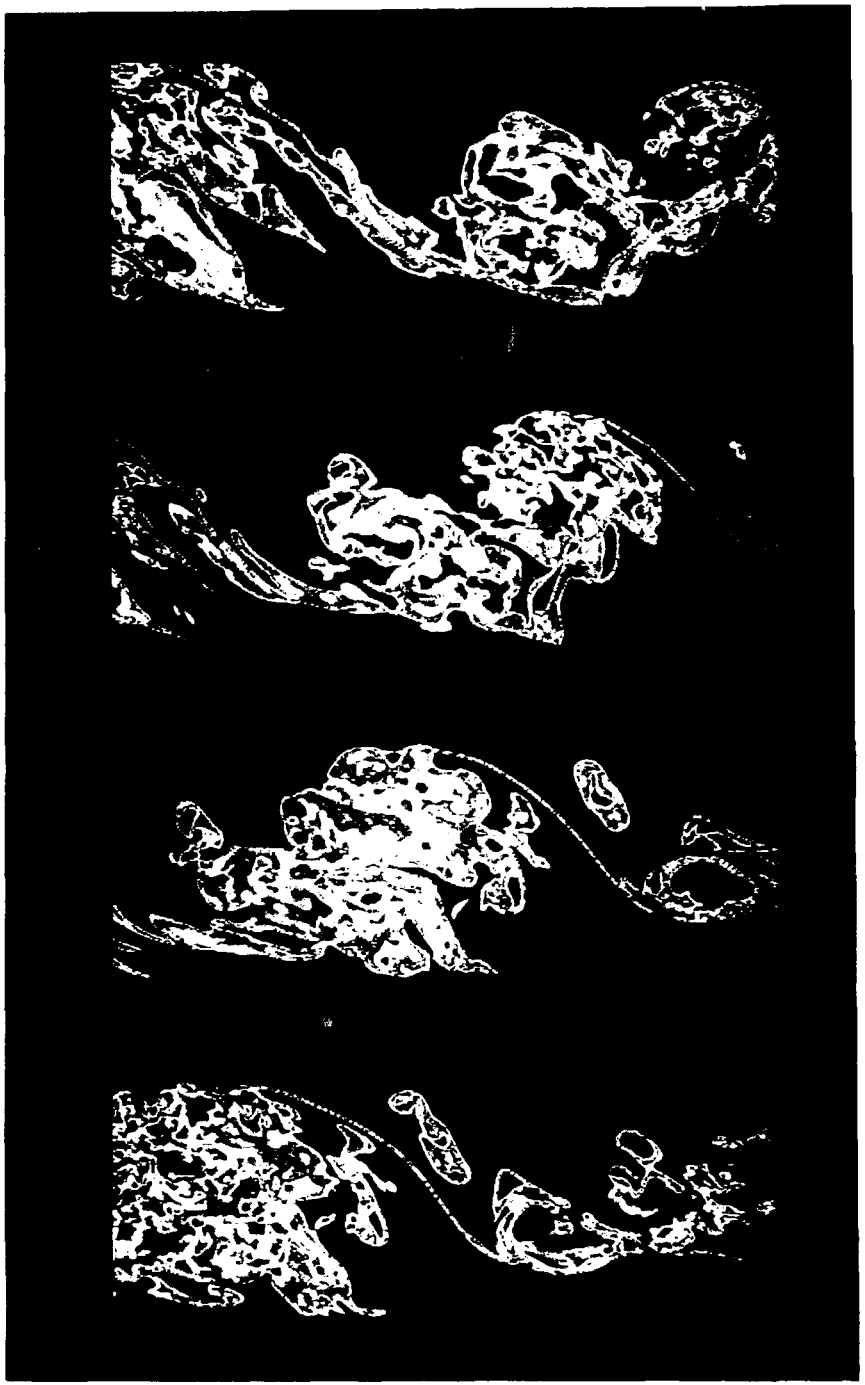

Figure 6

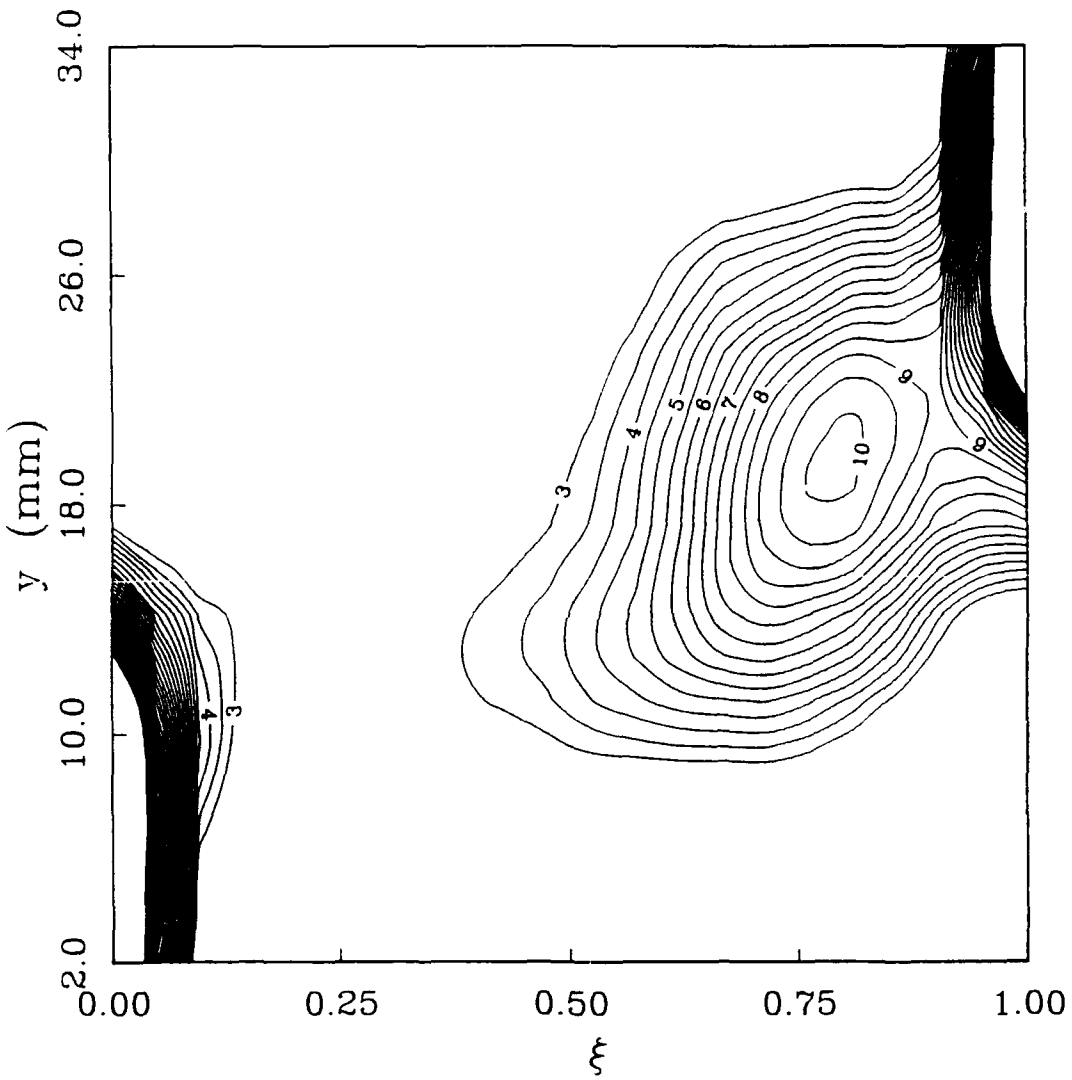

Figure 7a.

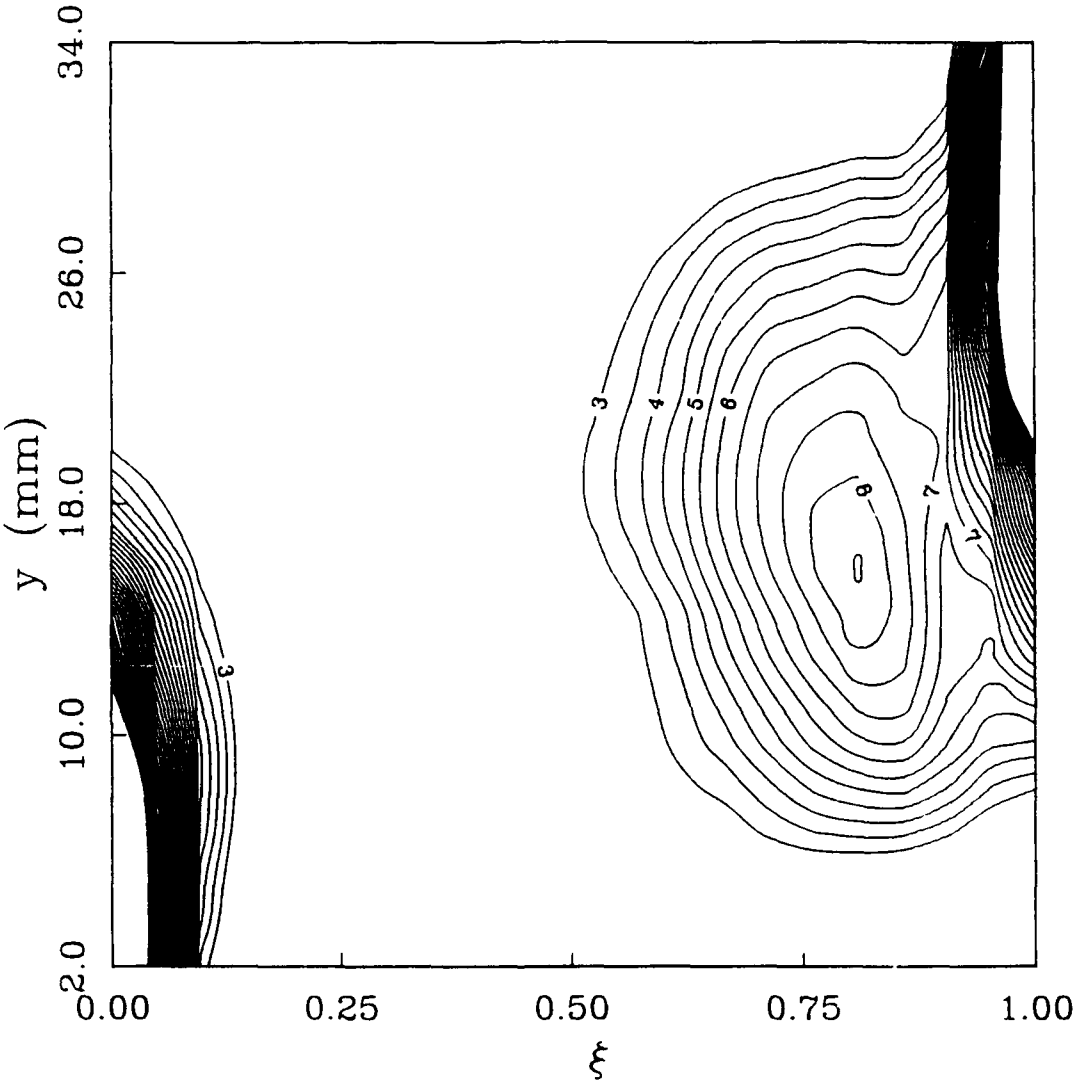

Figure 7b.

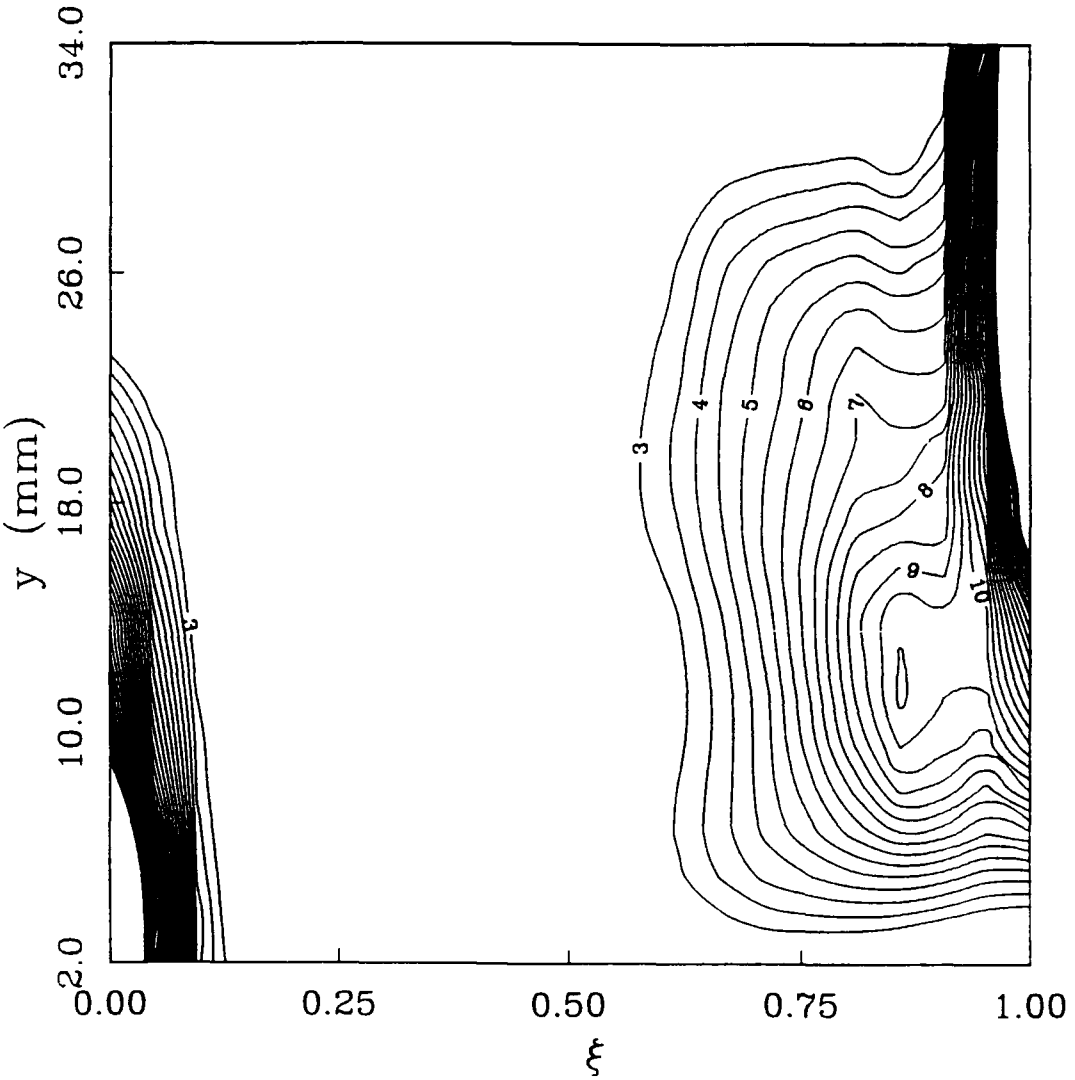

Figure 7c.

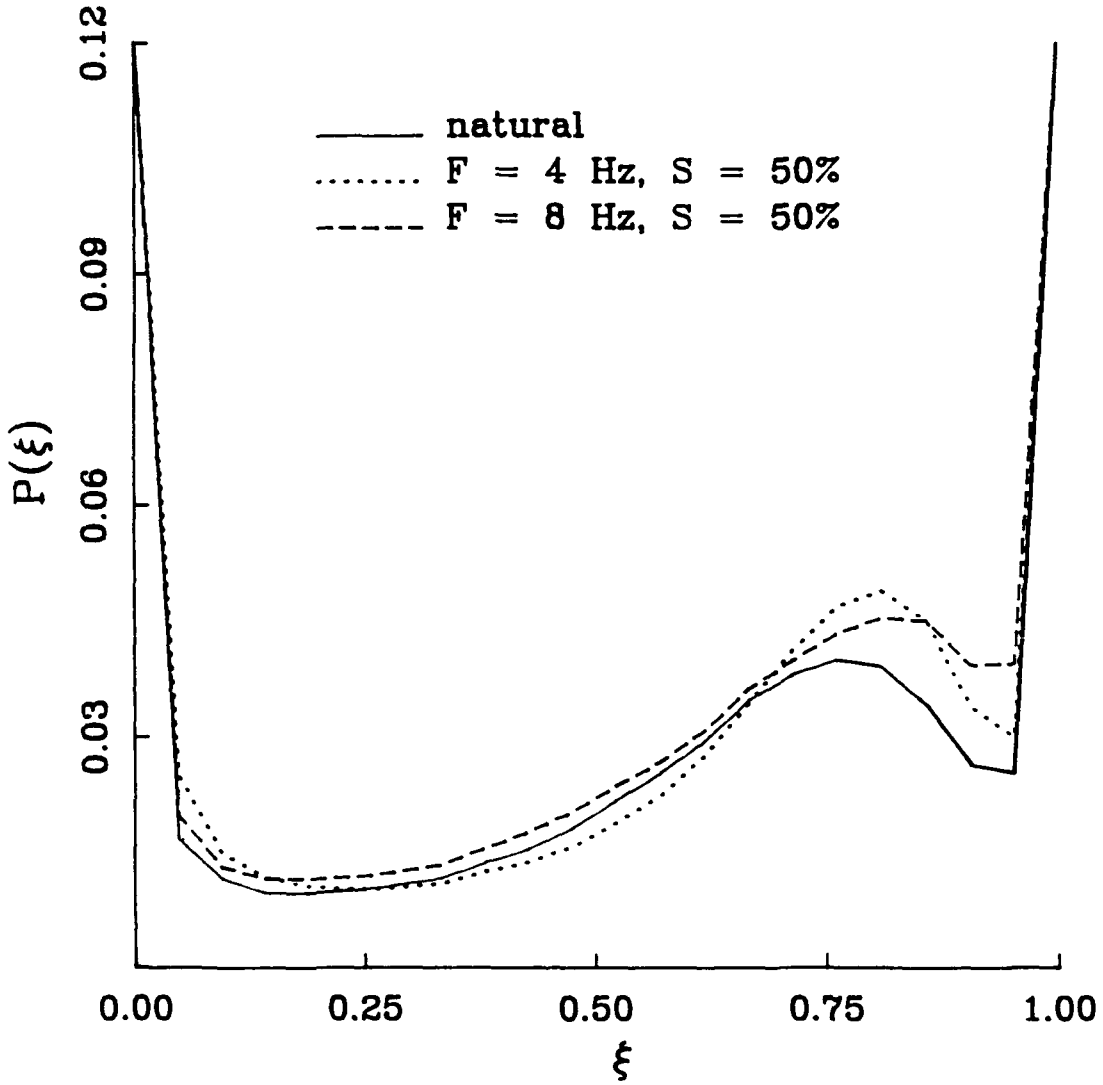
natural
F = 4 Hz, S = 50%
F = 8 Hz, S = 50%
P(ξ)
0.12
0.09
0.06
0.03
0.00
0.25
0.50
0.75
1.00
ξ

Figure 8a.

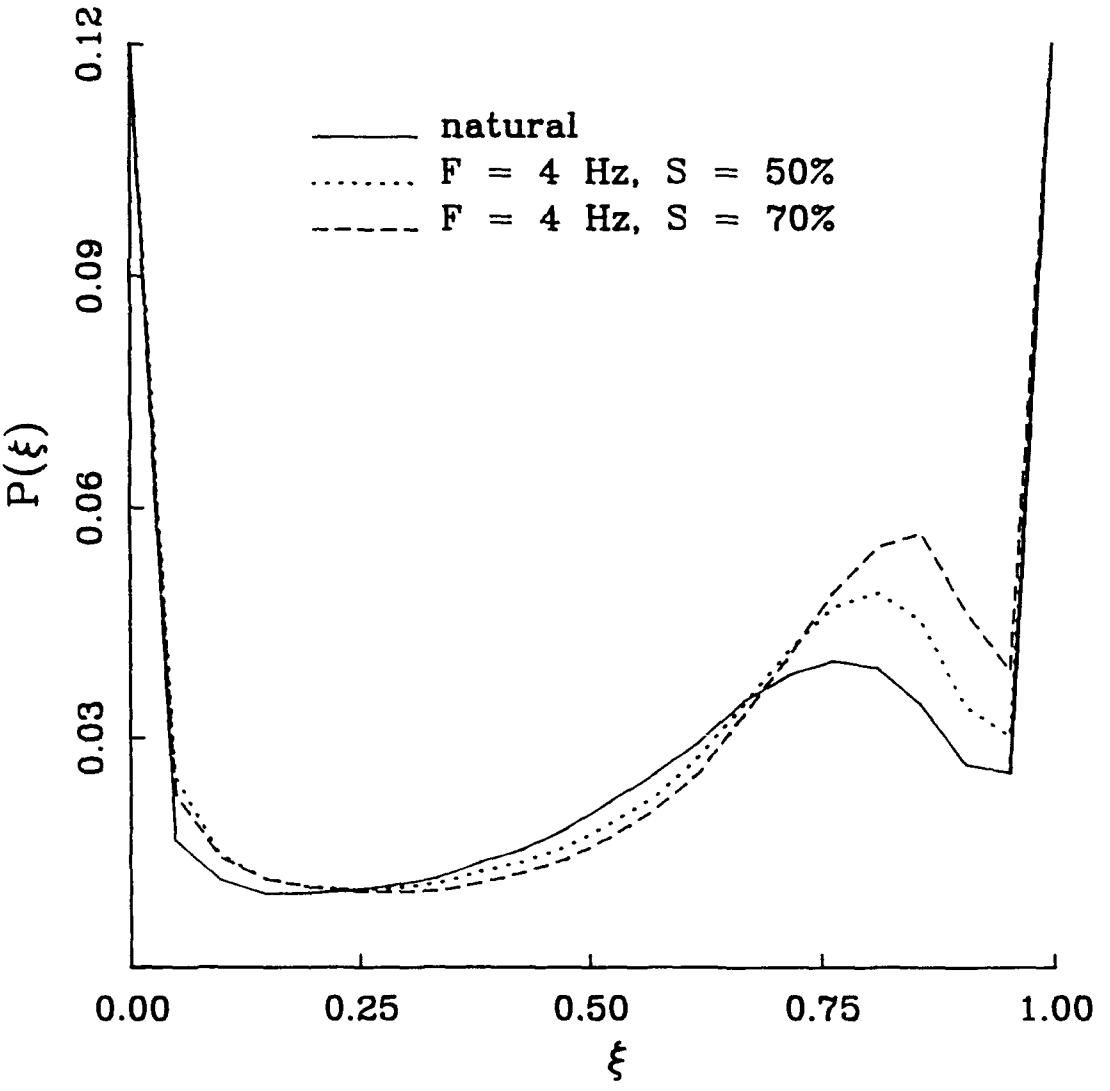
natural
F = 4 Hz, S = 50%
F = 4 Hz, S = 70%
P(ξ)
0.12
0.09
0.06
0.03
0.00
0.25
0.50
0.75
1.00
ξ

Figure 8b.

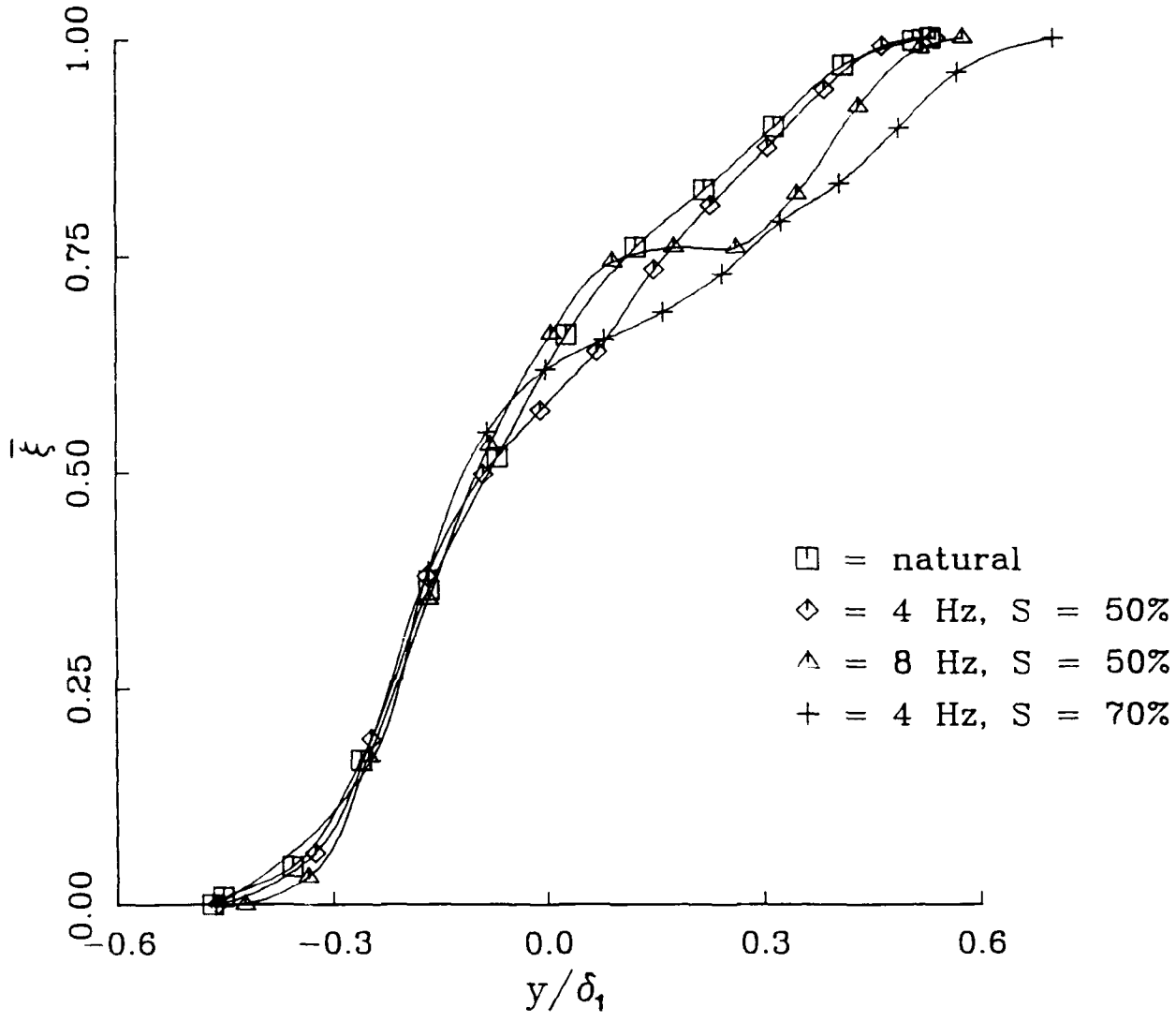
1.00
0.75
0.50
0.25
0.00
$\overline{\xi}$
−0.6
−0.3
0.0
0.3
0.6
y/δ_1
= natural
= 4 Hz, S = 50%
= 8 Hz, S = 50%
= 4 Hz, S = 70%

Figure 9.

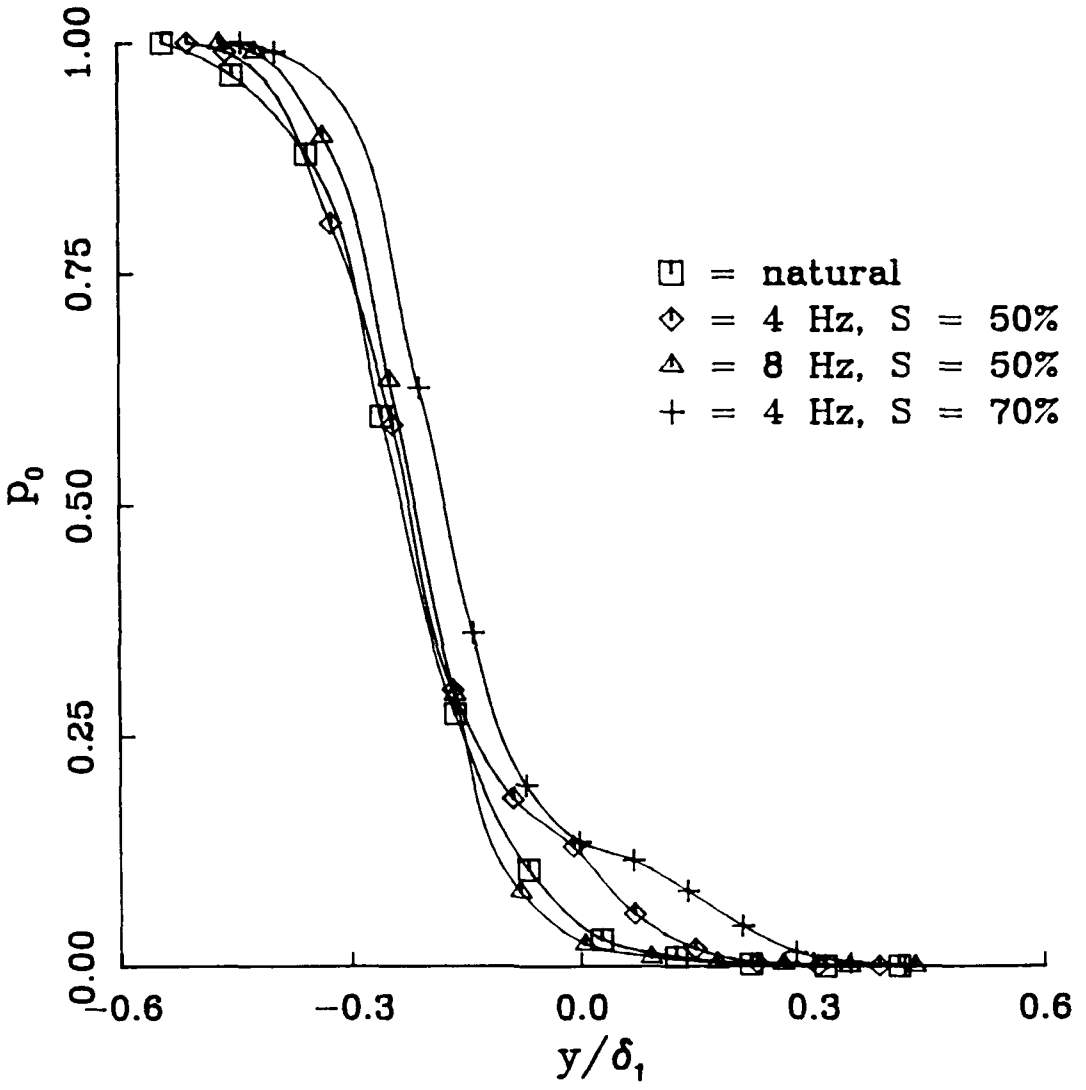
1.00
0.75
0.50
0.25
0.00
P_0
-0.6
-0.3
0.0
0.3
0.6
y/δ_1
□ = natural
◇ = 4 Hz, S = 50%
△ = 8 Hz, S = 50%
+ = 4 Hz, S = 70%

Figure 10a.

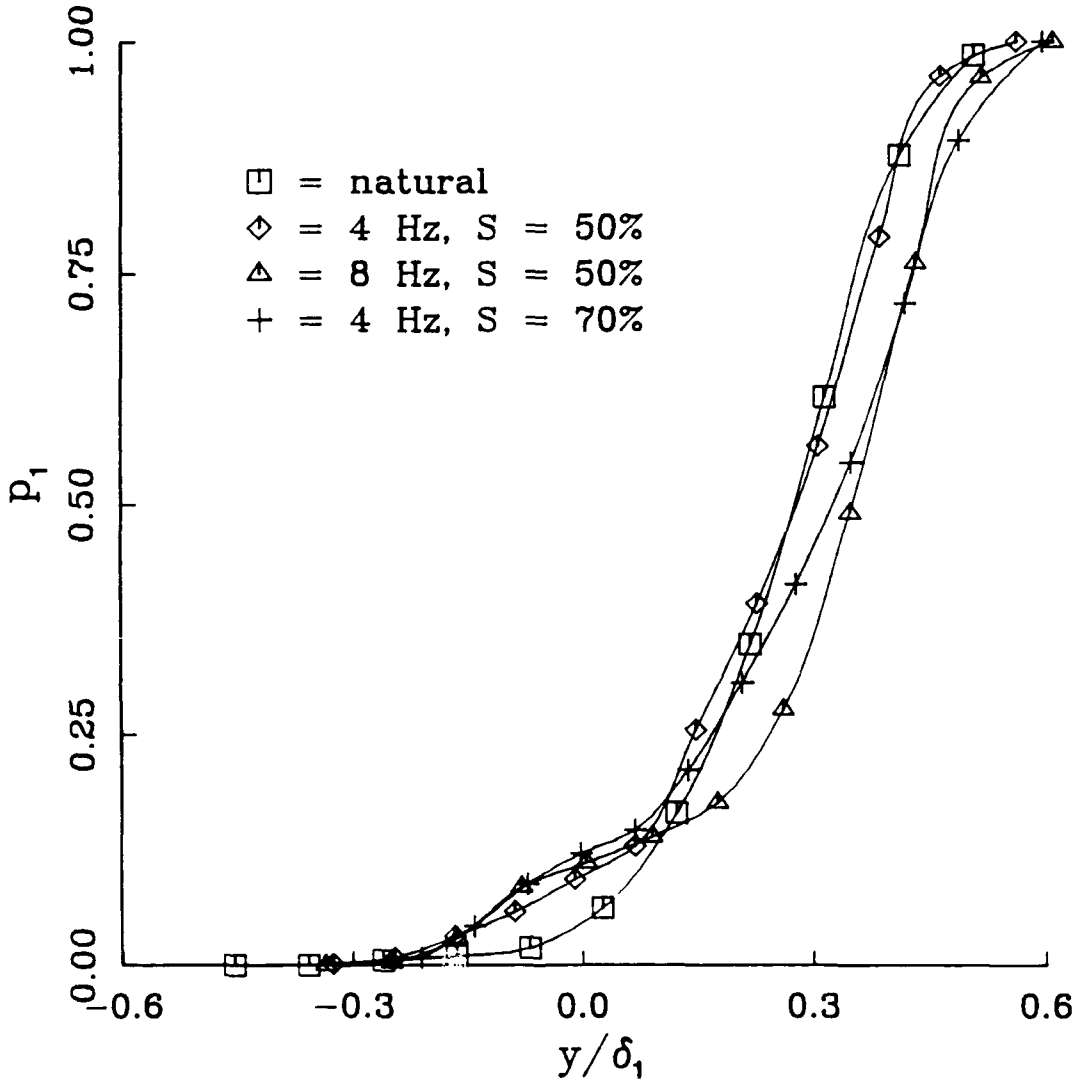
□ = natural
◇ = 4 Hz, S = 50%
△ = 8 Hz, S = 50%
+ = 4 Hz, S = 70%
P1
0.00
0.25
0.50
0.75
1.00
−0.6
−0.3
0.0
0.3
0.6
y/δ1

Figure 10b.

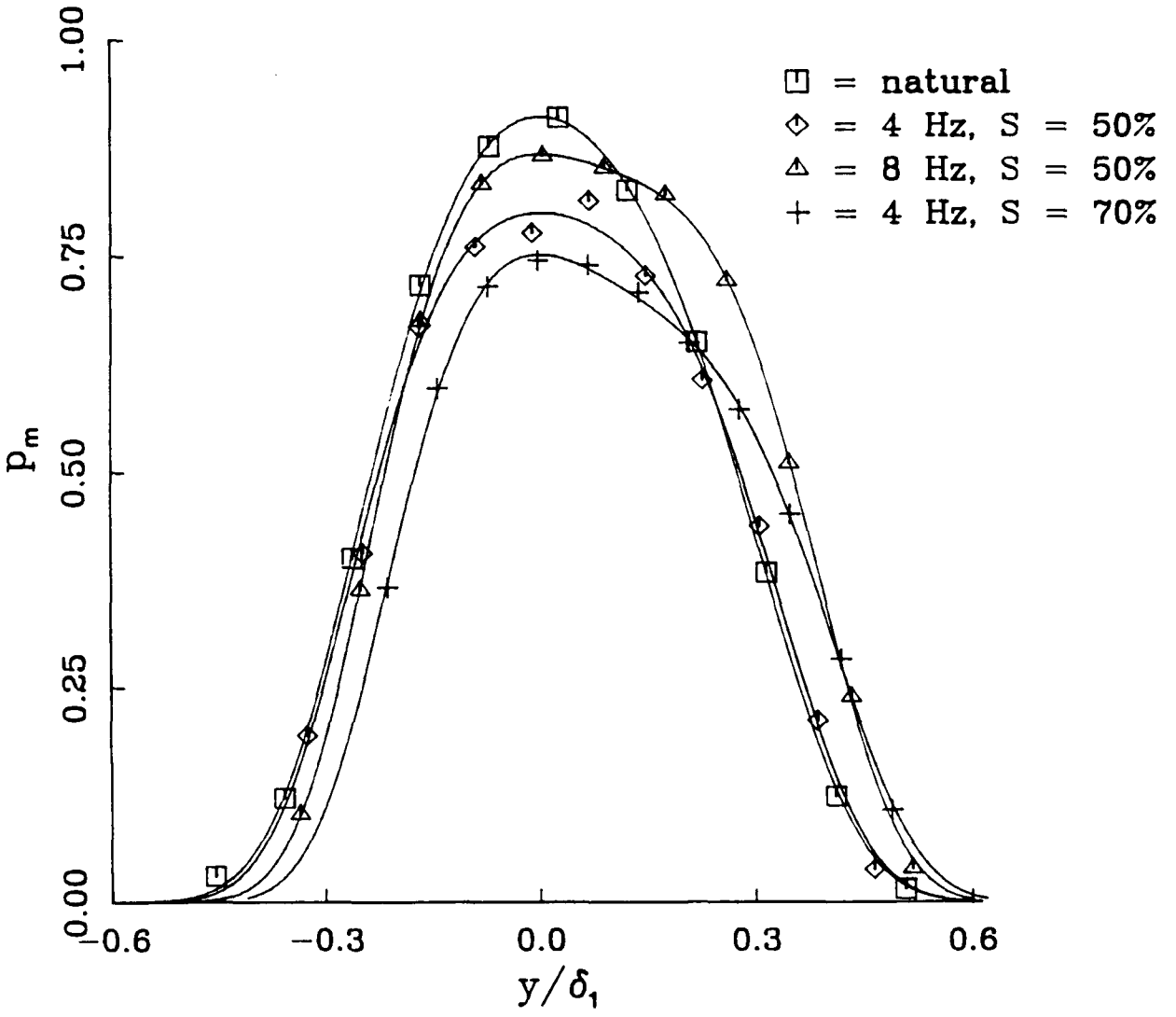
1.00
0.75
0.50
0.25
0.00
p_m
−0.6
−0.3
0.0
0.3
0.6
y/δ_1
□ = natural
◇ = 4 Hz, S = 50%
△ = 8 Hz, S = 50%
+ = 4 Hz, S = 70%

Figure 11.

APPENDIX B

EFFECTS OF EXTERNAL FORCING ON ENTRAINMENT RATIO AND FLUID COMPOSITION IN TURBULENT SHEAR LAYERS

by

M. M. Koochesfahani [#] and C. G. Mackinnon [*]

AFOSR Grant No. AFOSR-87-0332

Progress Report

20-March-1990

[#] Assistant Professor, Department of Mechanical Engineering, Michigan State University.

[*] Graduate Assistant, Department of Mechanical Engineering, Michigan State University.

1. INFLUENCE OF FORCING ON THE COMPOSITION OF MIXED FLUID IN A TWO-STREAM SHEAR LAYER

It is well documented that forcing can greatly modify the behavior of turbulent plane mixing layers [1-6]. While most of the research in this area has concentrated on the effects of forcing on the velocity field and layer growth rate, the modification of the *molecular* mixing field has received much less attention. Roberts [4,5] has shown that the extent of molecular mixing, as manifested by the amount of chemical product formed in the layer, can be altered by shear layer excitation. It is not known, at this time, how the composition distribution of the molecularly-mixed fluid in a shear layer is affected upon forcing. It is important to note that manipulating a turbulent shear layer to have more mixed fluid may be ineffective if the resulting mixed fluid has an undesirable composition. It is the purpose of this study to determine how the probability density function (*pdf*) of the concentration field is affected when a turbulent shear layer is forced. The investigation naturally addresses the behavior of both the large scale (2-D) entrainment and the small scale (3-D) structure of the forced flow since they determine the distribution of mixed fluid in the layer.

We are conducting experiments in a gravity-driven liquid shear layer facility where forcing is achieved by oscillating one of the two free-stream velocities using an oscillating bellows mechanism in one of the supply lines [7]. Utilizing laser induced fluorescence (LIF) diagnostics [8], we monitor the relative concentration of high-speed to low-speed fluid in the shear layer in terms of high-speed fluid volume fraction ξ. For the results described here, the shear free-stream speeds were set to U_1 = 40 cm/s, U_2 = 20 cm/s. The fluorescence intensity over a plane illuminated by a laser sheet was recorded by a 2-D, CCD array with a spatial resolution of 200 μm and temporal resolution of 2 msec at 60 fields/s. The array output was digitized to 8 bits at full video rate into hard disk in real time by a digital image acquisition system (TRAPIX-5500). Typically 240 sequential LIF images (i.e. 60 MBytes of data) were acquired to ensure the reliability of statistics and also allow the monitoring of the spatiotemporal evolution of the concentration field in two dimensions. These digital images provide spatially and temporally resolved concentration data at about 50,000 (simultaneous) points over a plane in the shear layer as a function of time.

We present in Figures 1 through 3 the effect of forcing on the shear layer structure. Each figure shows a time sequence (Δt = 1/15 sec) of the mixing field over a downstream region 16.7 cm < x < 24.5 cm. At each time step, the image is actually composed of 40,000 (100 in y and 400 in x) point measurements of concentration which have been used to calculate a simulated fast chemical reaction at unity equivalence ratio. The flow patterns for the case of sinusoidal forcing (symmetry

S = 50%) shown in Figure 2 are similar to those previously observed [4,5]. We note, however, that the shape of the forcing waveform has a dramatic influence on the flow (see Figure 3). The case shown in Figure 3 illustrates that using an asymmetric waveform with S = 70% results in a larger growth rate than sinusoidal forcing (Fig. 2, 4 *Hz* case), whereas S = 30% produces a "forced" layer which is more similar to a "natural" layer.

Figures 4, 5 demonstrate the effects of forcing on the *pdf* of the mixed-fluid concentration field $P(\xi)$ at a downstream distance of about x = 21 cm. At this location, the Reynolds number of the natural layer, based on the visual thickness and the velocity difference, is about 6,000 which corresponds to a turbulent mixing layer during the mixing transition. The most striking result is that *both the amount and the composition* of mixed fluid are modified upon external forcing. For the cases we have studied thus far, the predominant concentration shifts to larger values and the total amount of mixed fluid increases (Fig. 4a). Another important finding is that the details of the forcing waveform shape have a significant influence on the mixing field (Fig. 4b). At the same forcing frequency, changing the symmetry of the waveform alters both the amount and the composition of the mixed-fluid. In Figure 5, we show how waveform shaping can lead to either major (Fig. 5a) or minor (Fig. 5b) changes in the mixed-fluid composition field.

The changes in the mixed-fluid *pdf* reported here can be the result of modification to three processes: (1) the engulfment of the free-stream fluids in the first rolled-up vortex (or vortices), (2) the overall, 2-D entrainment field into the layer farther downstream beyond the first roll-up location, and (3) development of streamwise vortices and 3-D small scales. We are in the process of isolating these three effects by making concentration measurements in the early stages of vortex formation and by studying the spanwise structure of the forced flow (both visualization and concentration measurements).

2. EFFECT OF CURVATURE ON MOLECULAR MIXING IN A TWO-STREAM SHEAR LAYER

In a separate smaller effort, we are studying how shear layer curvature may affect molecular mixing. The extensive body of knowledge which exists on turbulent flow curvature effects concentrates on the characterization of the velocity field (see, for example, Ref. 9) whereas much less is known about the mixing field. Besides the inherent interest in curvature effects on fluid mechanics phenomena, use of curvature as a possible tool for (molecular) mixing control needs to be investigated. Curvature could change the mixing field by modifying the overall large scale (2-D) entrainment into the flow and also by changes in the 3-D structure of the flow due to the Taylor-Goertler instability. The study we describe below outlines the portion of our work on the effects of curvature on the 2-D structure of the shear layer. We are planning to also address 3-D effects which may be the most important mechnism through which curvature modifies the mixing field.

We investigated the effect of curvature on the 2-D structure of a shear layer both theoretically and experimentally. The inviscid, linear, parallel-flow stability analysis of spatially growing disturbances [10,11] was utilized to study the instability characteristics of a curved shear layer. It can be shown that, for a curved layer, the disturbance eigenfunction, ϕ, satisfies the modified Rayleigh equation given by

$$\phi'' + \frac{1}{R}\phi' - \left[\alpha^2 + \frac{U'' + U'/R - U/R^2}{U - \beta/\alpha}\right]\phi = 0$$

where $(\,)''$ corresponds to d^2/dy^2, $(\,)'$ to d/dy and $U(y)$ is the mean velocity profile. In the equation above, $\alpha = \alpha_r + i\alpha_i$ is the complex non-dimensional wave-number and β is the non-dimensional frequency which is taken as pure real for the present spatial calculations. The nondimensional radius of curvature is given by $R = \rho/\delta$ where ρ is the (dimensional) radius of curvature and δ is the shear layer thickness. A positive value of R corresponds to the high-speed stream on the outside whereas a negative value implies that the high-speed stream is on the inside of the curved layer. We use a mean velocity profile which incorporates the initial wake component near the splitter plate. The form of the velocity profile and the solution method for obtaining the values of unstable α, β, and the corresponding shape of the eigenfunction $\phi(y)$ are similar to those described in Reference 11 and will not be repeated here.

The effect of curvature on the instability characteristics of a $r = U_1/U_2 = 3$ shear layer (i.e. $\lambda = (r-1)/(r+1) = 0.5$) is shown in Figures 6 and 7. In these

figures, the curvature value of $R = 100$ is large enough to represent the limit of a straight shear layer (i.e. no curvature). Similar to previous results [11], two modes of instability are found. Mode one (the shear layer mode) leads to the usual Kelvin-Helmholtz shear layer rollup, whereas mode 2 (the wake mode) rollup pattern resembles a wake flow. We note that the effect of curvature (positive or negative) is minimal even at a curvature as small as 10. Similar conclusion is reached when we examine the vorticity eigenfunction (i.e. vorticity mode shape) at maximum amplification (see Figure 8).

To study curvature effects experimentally, the shear layer facility was modified to accommodate a curved test section. Visualization of the flow patterns for natural and forced conditions is shown in Figure 9. The similarity between straight and curved shear layers, both natural and forced, supports the conclusions reached based on the sability analysis.

Our results to date indicate that curvature may not play any major role in modifying the initial development of the shear layer vortices and the fluid entrained into them. The influence of curvature on streamwise vorticity is known to be very strong. How this affects the molecular mixing field remains to be shown.

3. REFERENCES

1. Ho, C-M. and Huang, L-S., "Subharmonics and vortex merging in mixing layers," *J. Fluid Mech.*, **119**, 1982, pp. 443-473.
2. Oster, D. and Wygnanski, I., "The forced mixing layer between parallel streams," *J. Fluid Mech.*, **123**, 1982, pp. 91-130.
3. Ho, C-M. and Huerre, P., "Perturbed free shear layers," *Ann. Rev. Fluid Mech.*, **16**, 1984, pp. 365-424.
4. Roberts, F. A., "Effects of a periodic disturbance on mixing in turbulent shear layers and wakes," Ph.D. Thesis, California Institute of Technology, 1985.
5. Roberts, F. A. and Roshko, A., "Effects of periodic forcing on mixing in turbulent shear layers and wakes," AIAA-85-0570, 1985.
6. Koochesfahani, M. M. and Dimotakis, P. E., "Effects of a downstream disturbance on the structure of a turbulent plane mixing layer," *AIAA J.*,**27(2)**, 1989, pp. 161-166.
7. Koochesfahani, M. M., "Effects of external forcing on entrainment ratio and fluid composition in turbulent shear layers," AFOSR-87-0332 Annual Progress Report, 31-August-1988.
8. Koochesfahani, M. M. and Dimotakis, P. E., "Laser induced fluorescence measurements of mixed fluid concentration in a liquid plane shear layer," *AIAA J.*, **23(11)**, 1985, pp. 1700-1707.
9. Wang, Chiun, "The effects of curvature on turbulent mixing layers," Ph.D. Thesis, California Institute of Technology, 1984.
10. Michalke, A., "On spatially growing disturbances in an inviscid shear layer", *J. Fluid Mech.*, **23(3)**, 1965, pp. 521-544.
11. Koochesfahani, M. M. and Frieler, C. E., "Instability of nonuniform density free shear layers with a wake profile," *AIAA J.*, **27(12)**, 1989, pp. 1735-1740.

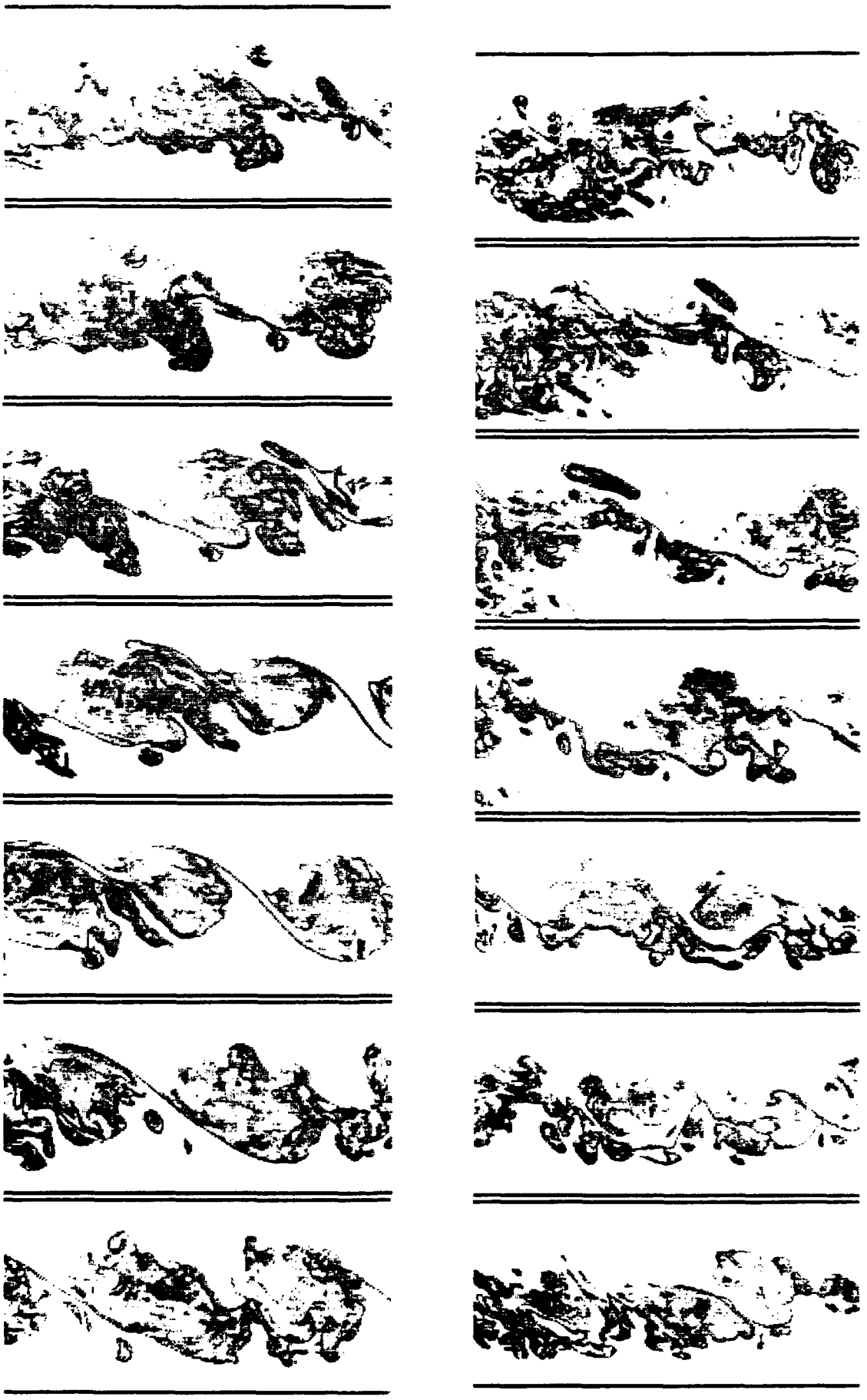

Figure 1. Digital image time sequence of the mixing field for the natural shear layer. Flow is from right to left and time increases from top to bottom. Two different time sequences are shown to indicate that the large scale organization of the flow is not always apparent.

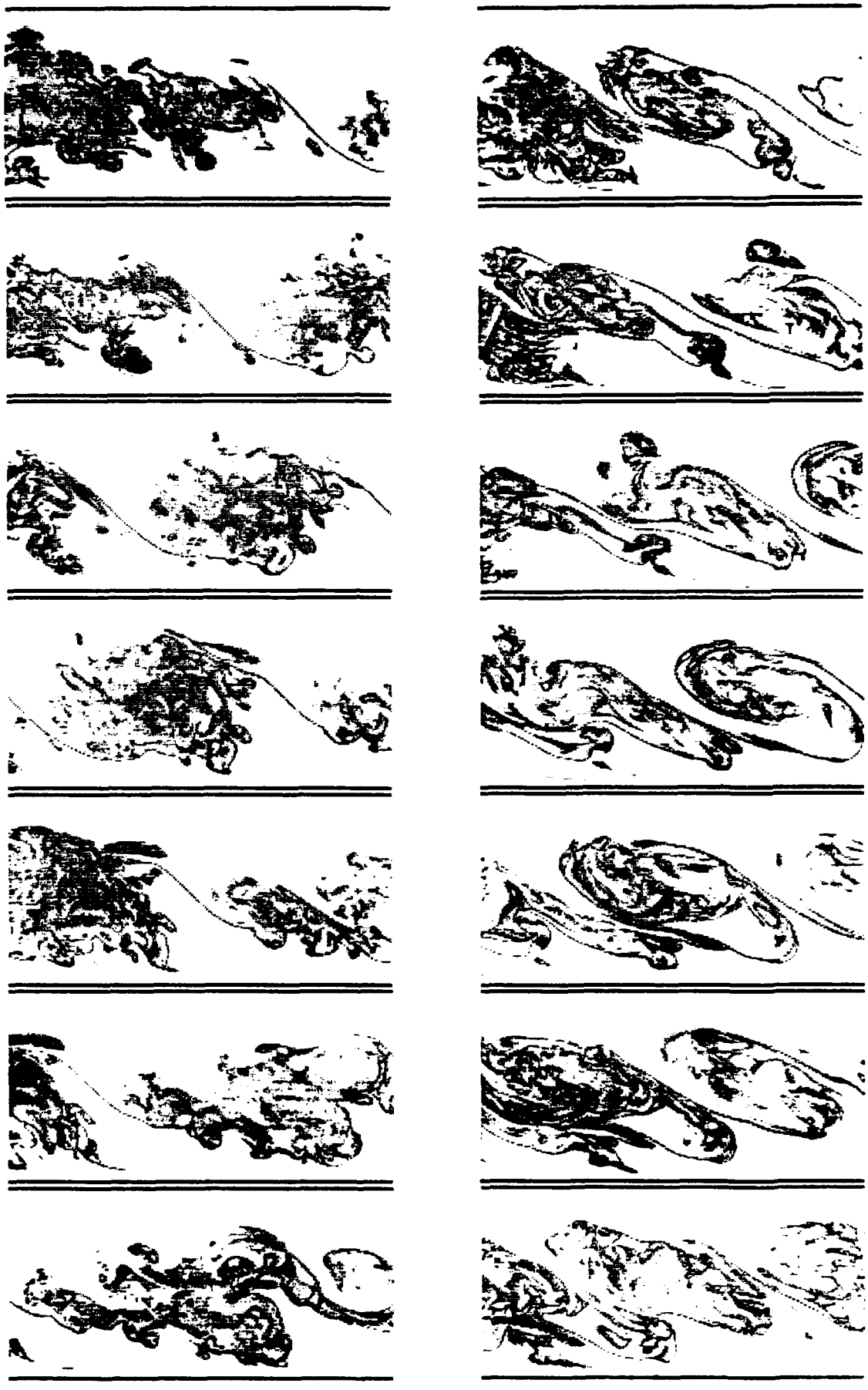

F = 4 Hz *F = 8 Hz*

Figure 2. Digital image time sequence of the mixing field for sinusoidal forcing. The shear layer natural frequency at the splitter plate tip is about $F_o \approx 27$ Hz.

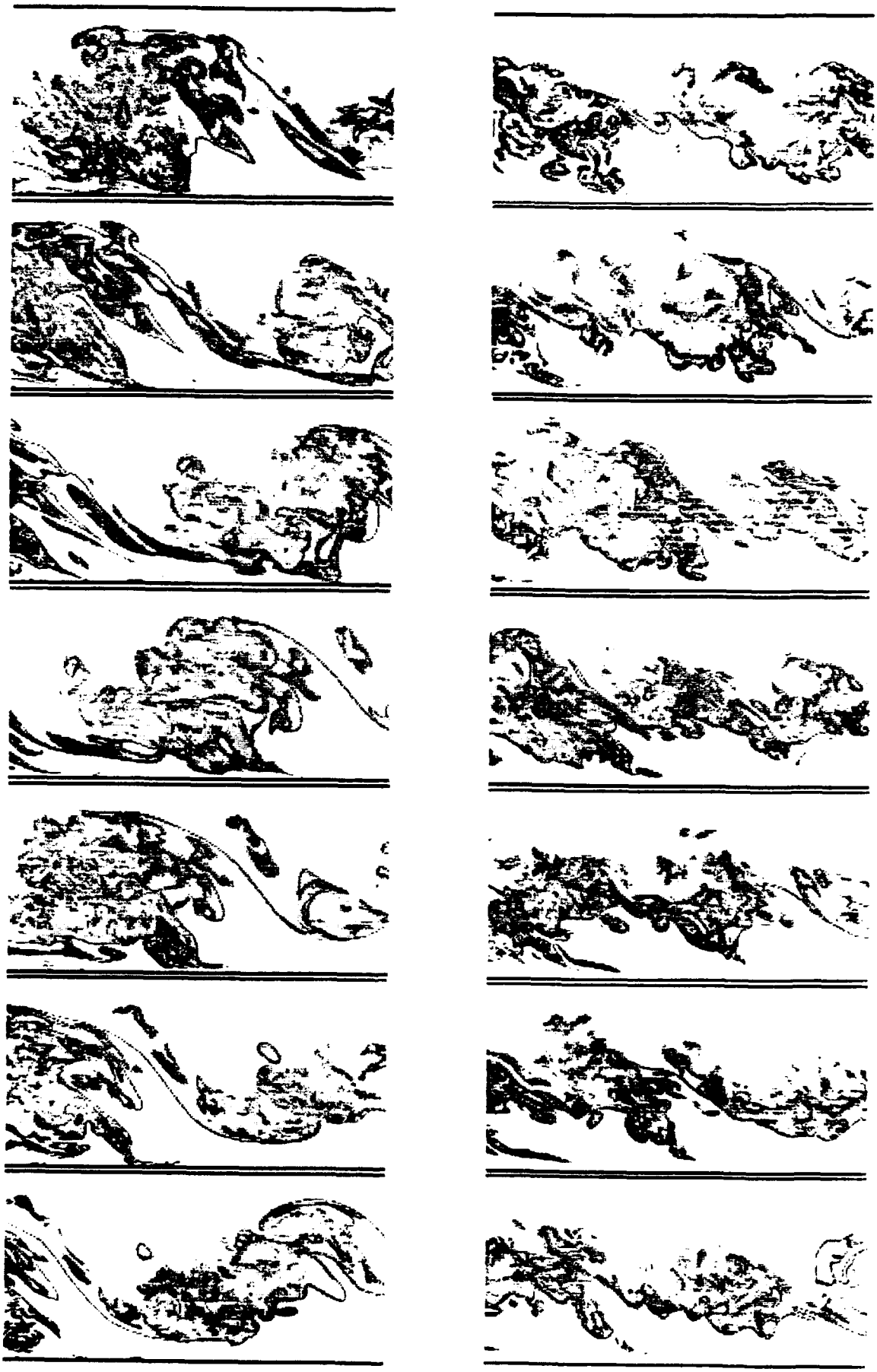

Figure 3. Digital image time sequence of the mixing field for nonsinusoidal forcing at $F = 4$ Hz.

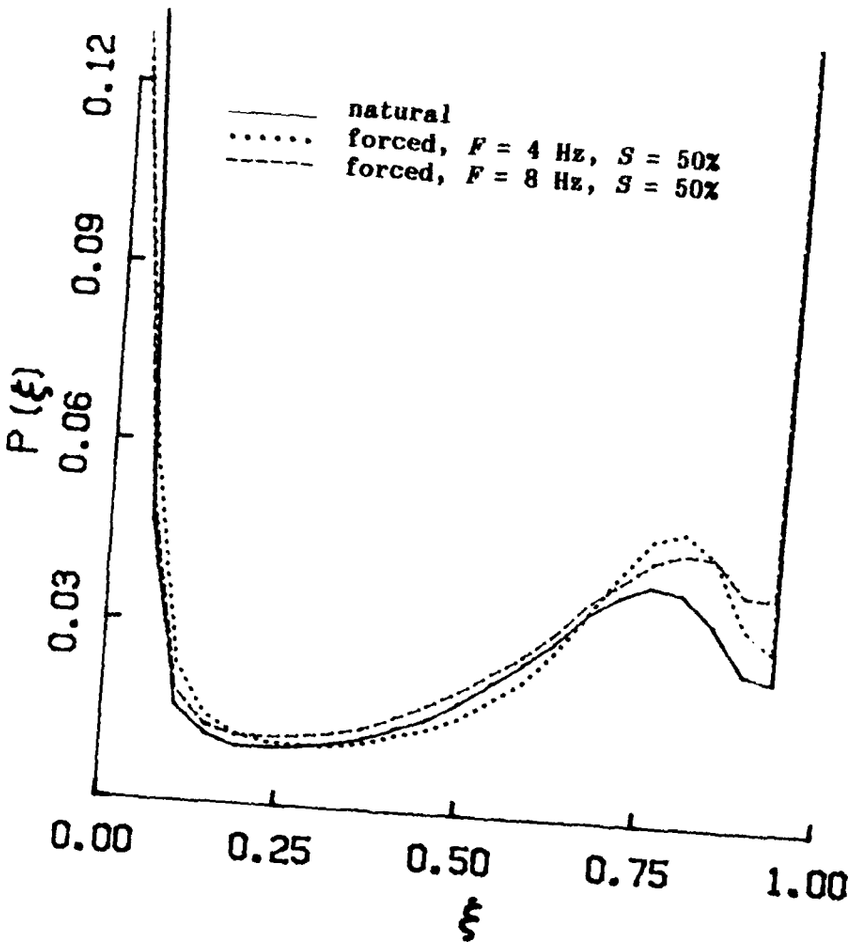

(a) Sinusoidal forcing

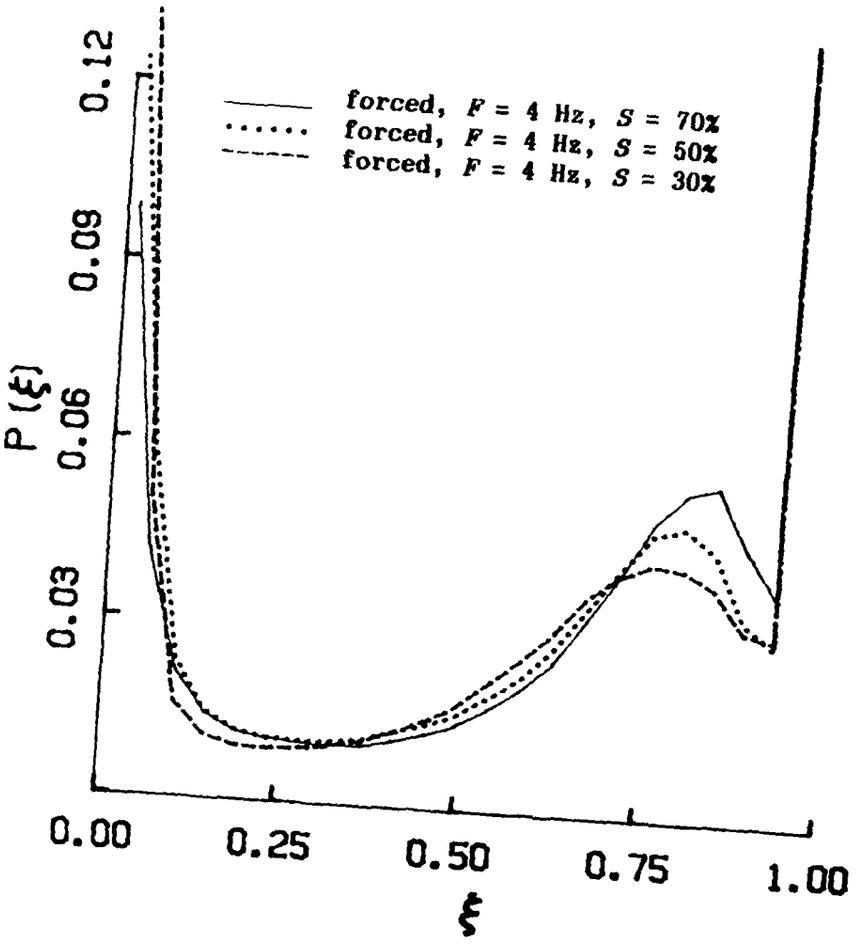

(b) Nonsinusoidal forcing

Figure 4. Effect of forcing on the *pdf* of the concentration field.

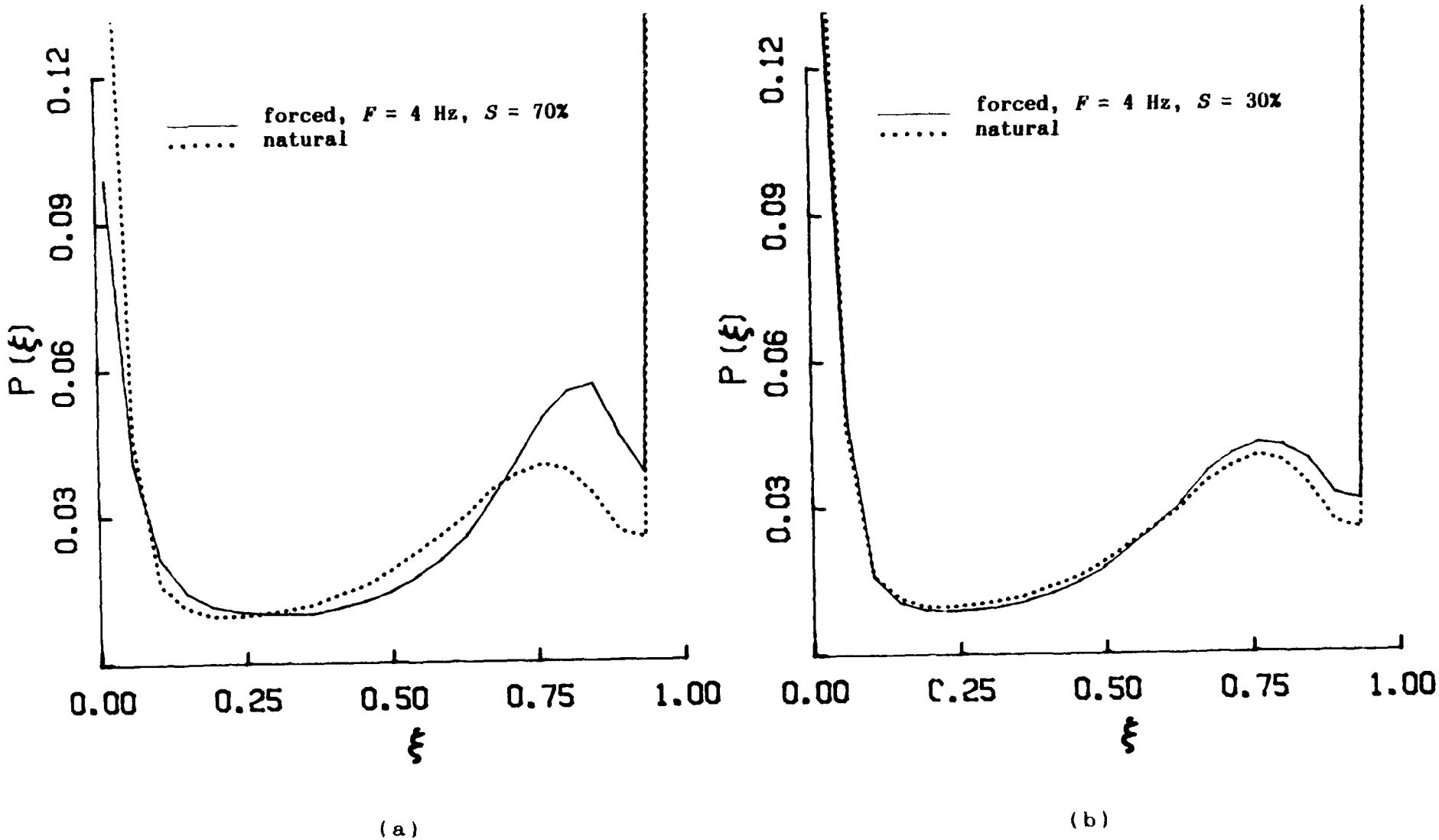

Figure 5. Control of the forcing waveform asymmetry can be used to make a major or minor modification in the mixed-fluid *pdf*.

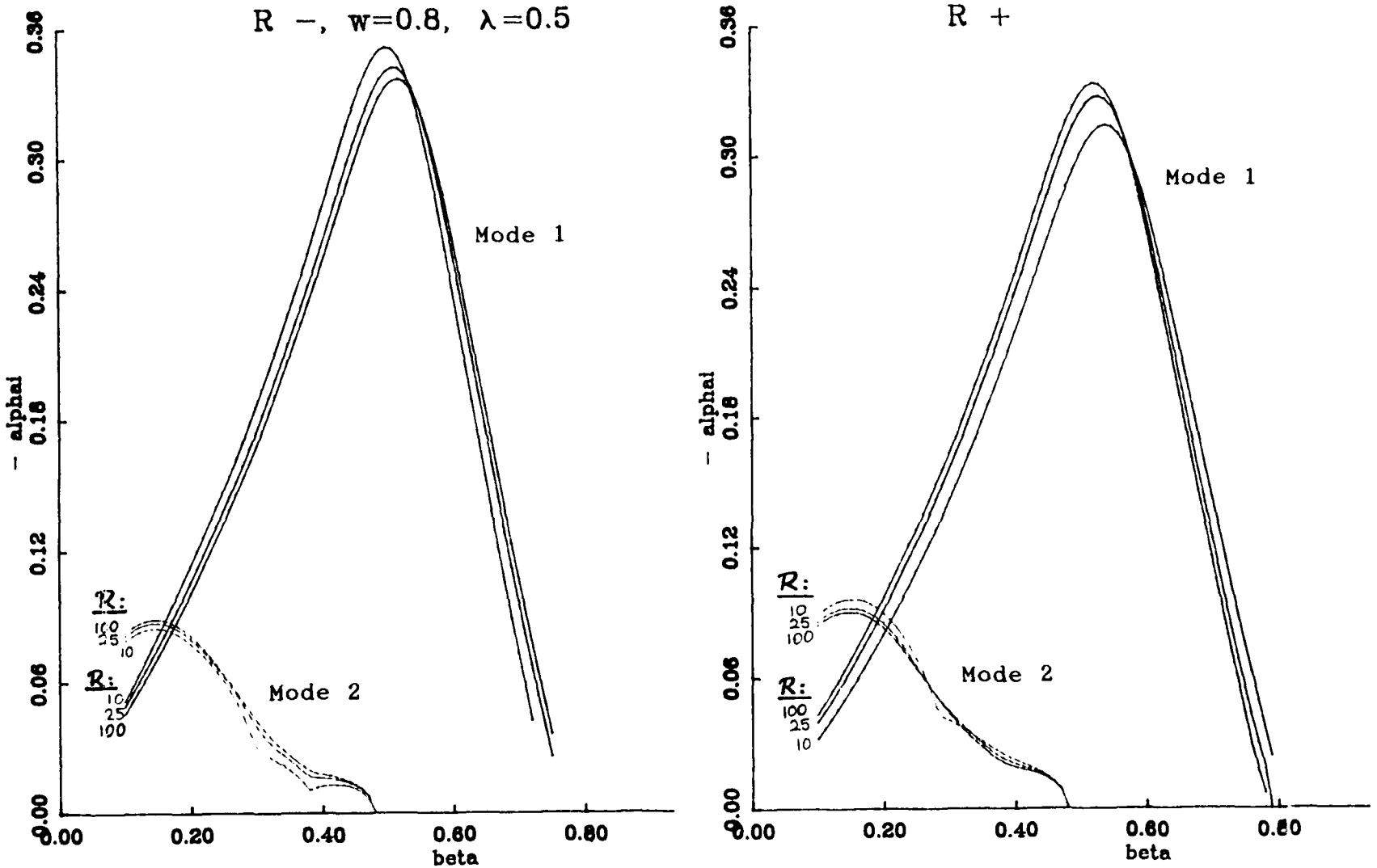

Figure 6. Effect of curvature on the amplification rate ($-\alpha_i$) of instability. Modes 1 and 2 correspond to the shear layer and wake modes, respectively. Positive/negative curvature corresponds to the high-speed stream on the outside/inside of the curved layer. The straight (infinite R) shear layer limit is represented by the curves for $R = 100$.

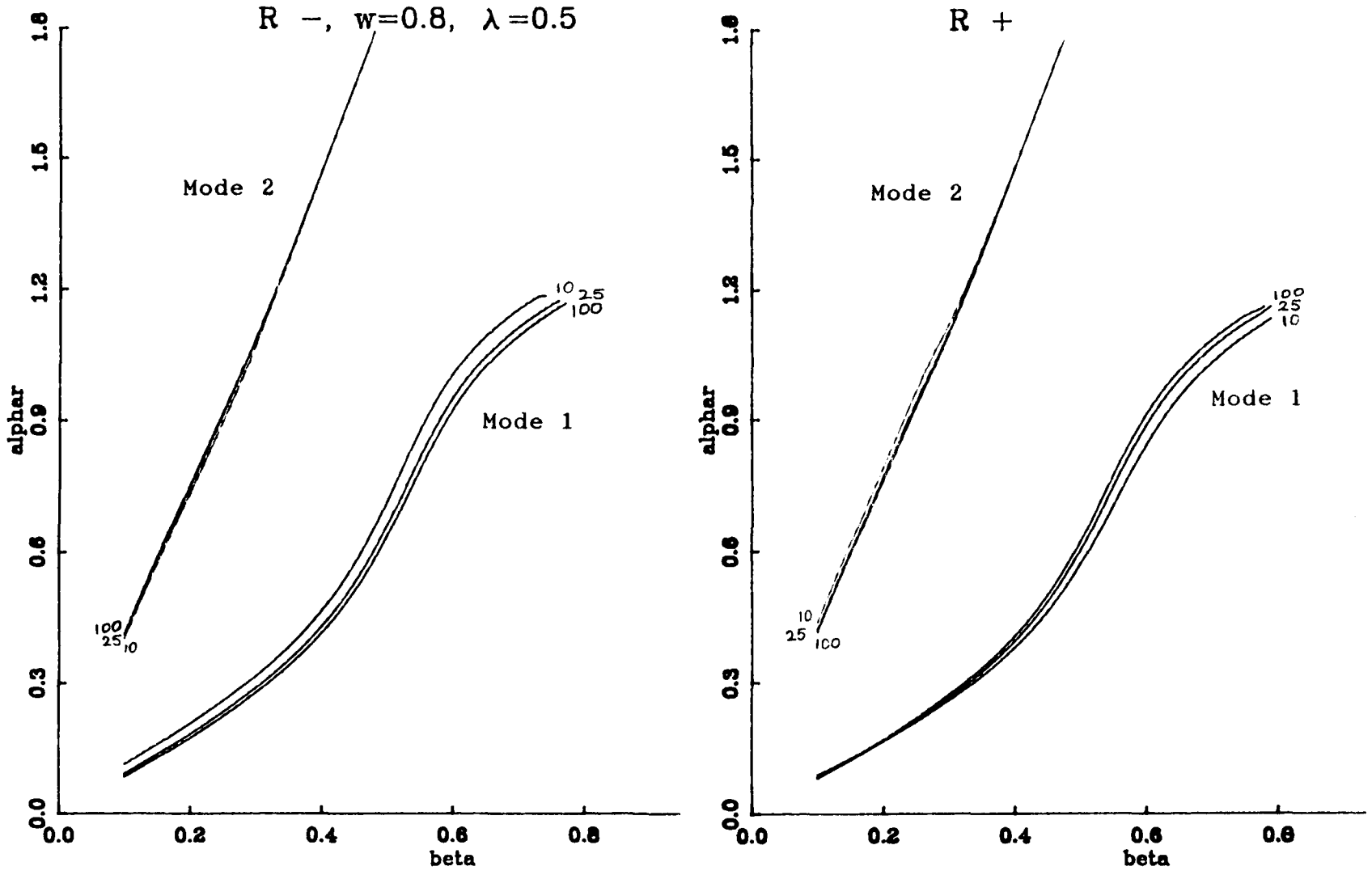

Figure 7. Effect of curvature on the wavenumber (α_r) of instability. Modes 1 and 2 correspond to the shear layer and wakes modes, respectively. Positive/negative curvature corresponds to the high-speed stream on the outside/inside of the curved layer. The straight (infinite R) shear layer limit is represented by the curves for $R = 100$.

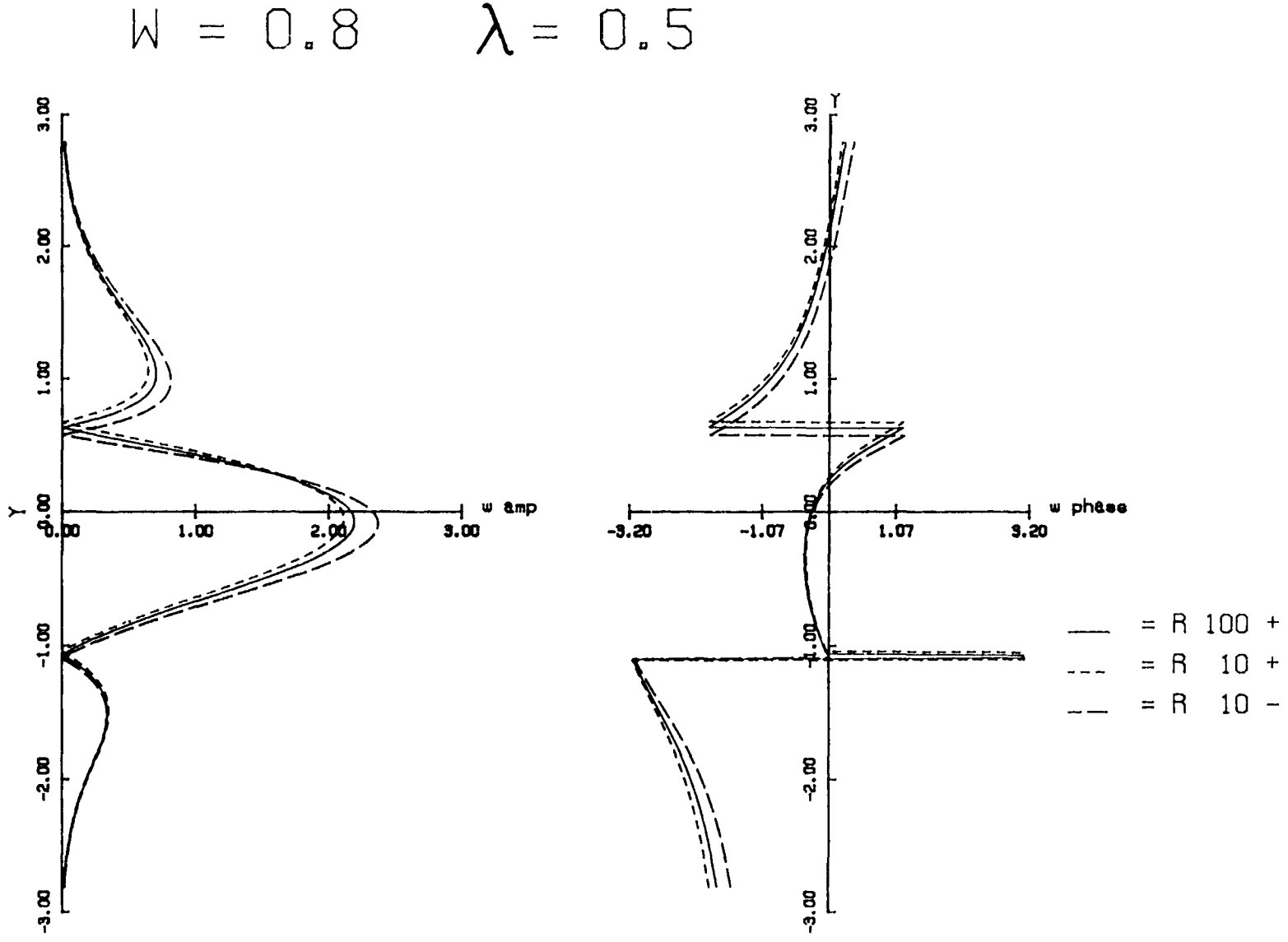

Figure 8. Effect of curvature on the vorticity eigenfunction at maximum amplification rate.

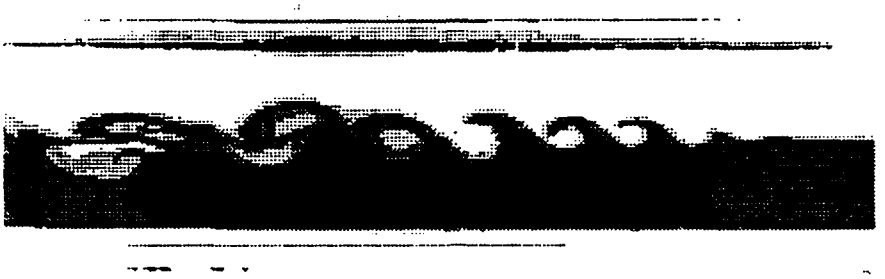

Straight shear layer

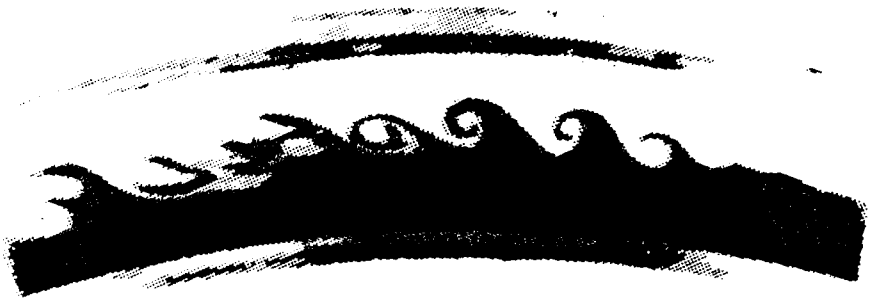

Curved shear layer

(a) Digital LIF images of the natural shear layer. $U_1 = 10$ cm/s, $U_2 = 5$ cm/s

Straight shear layer [7]

Curved shear layer

(b) LIF images of the shear layer forced at near natural frequency.

Figure 9. Flow visualization in a curved shear layer.